linker between membrane-located receptors and cytoskeleton, primarily affecting cell motility and invasion (11, 12). In this study, corresponding to enhanced cell motility, co-localized cortactin with actin filaments at lamellipodias or fillopodias was also observed in highly metastatic cells. Studies in normal cells have shown that cortactin was actively involved in lamellipodia actin polymerization (20–22). Lamellipodias and fillopodias are membrane structures formed during cell spreading and migration (35). It can be deduced from these reports that cortactin plays important roles in cell migration through its roles in integrin-stimulated actin cytoskeleton rearrangements during cancer metastasis. Support for this deduction is provided by the study of overexpression of cortactin in human tumors or NIH 3T3 fibroblasts, which has been shown to result in increased cell motility (36, 37). Overall, results in this study indicate that the Fyn-cortactin pathway is specifically activated for signaling of cell migration and spreading during the progression of cancer metastasis.

Identification of specific involvements of Fyn and cortactin in integrin signaling pathways in metastatic melanoma cell lines provided important information for the understanding of mechanisms underlying the progression of cancer metastasis. Further studies are necessary to elucidate what is produced *de novo* for the activation of Fyn and how it affects Fyn activity stimulated by integrin in metastasis. Moreover, to fully clarify their roles in metastasis and to provide further information for cancer therapy, the effect of blocking tyrosine phosphorylation of cortactin or suppressing expression of cortactin on the metastasis potential also needs to be further investigated.

Acknowledgments—We thank Dr. I. J. Fidler for kindly providing murine melanoma cell lines. We also thank Dr. I. Kitabayashi for mass spectrometry analysis.

REFERENCES

1. Bishop, J. M. (1987) *Science* **235,** 305–311
2. Fidler, I. J. (1990) *Cancer Res.* **50,** 6130–6138
3. Fincham, V. J., and Frame, M. C. (1998) *EMBO J.* **17,** 81–92
4. Cary, L. A., Klinghoffer, R. A., Sachsenmaier, C., and Cooper, J. A. (2002) *Mol. Cell. Biol.* **22,** 2427–2440
5. Boyer, B., Bourgeois, Y., and Poupon, M. F. (2002) *Oncogene* **21,** 2347–2356
6. Huang, J., Hamasaki, H., Nakamoto, T., Honda, H., Hirai, H., Saito, M., Takato, T., and Sakai, R. (2002) *J. Biol. Chem.* **277,** 27265–27272
7. LaVallee, T. M., Prudovsky, I. A., McMahon, G. A., Hu, X., and Maciag, T. (1998) *J. Cell Biol.* **141,** 1647–1658
8. Irby, R. B., Mao, W., Coppola, D., Kang, J., Loubeau, J. M., Trudeau, W., Karl, R., Fujita, D. J., Jove, R., and Yeatman, T. J. (1999) *Nat. Genet.* **21,** 187–190
9. Takayama, T., Mogi, Y., Kogawa, K., Yoshizaki, N., Muramatsu, H., Koike, K., Semba, K., Yamamoto, T., and Niitsu, Y. (1993) *Int. J. Cancer* **54,** 875–879
10. Schlaepfer, D. D., Hauck, C. R., and Sieg, D. J. (1999) *Prog. Biophys. Mol. Biol.* **71,** 435–478
11. Wu, H., and Parsons, J. T. (1993) *J. Cell Biol.* **120,** 1417–1426
12. van Damme, H., Brok, H., Schuuring-Scholtes, E., and Schuuring, E. (1997) *J. Biol. Chem.* **272,** 7374–7380
13. Huang, C., Liu, J., Haudenschild, C. C., and Zhan, X. (1998) *J. Biol. Chem.* **273,** 25770–25776
14. Schaller, M. D. (2001) *Oncogene* **20,** 6459–6472
15. Fidler, I. J., Gruys, E., Cifone, M. A., Barnes, Z., and Bucana, C. (1981) *J. Natl. Cancer Inst.* **67,** 947–956
16. Sakai, R., Iwamatsu, A., Hirano, N., Ogawa, S., Tanaka, T., Mano, H., Yazaki, Y., and Hirai, H. (1994) *EMBO J.* **13,** 3748–3756
17. Basara, M. L., McCarthy, J. B., Barnes, D. W., and Furcht, L. T. (1985) *Cancer Res.* **45,** 2487–2494
18. Hanke, J. H., Gardner, J. P., Dow, R. L., Changelian, P. S., Brissette, W. H., Weringer, E. J., Pollok, B. A., and Connelly, P. A. (1996) *J. Biol. Chem.* **271,** 695–701
19. Sakai, R., Nakamoto, T., Ozawa, K., Aizawa, S., and Hirai, H. (1997) *Oncogene* **14,** 1419–1426
20. Uruno, T., Liu, J., Zhang, P., Fan, Y., Egile, C., Li, R., Mueller, S. C., and Zhan, X. (2001) *Nat. Cell Biol.* **3,** 259–266
21. Kaksonen, M., Peng, H. B., and Rauvala, H. (2000) *J. Cell Sci.* ***113,*** 4421–4426
22. Wu, H., Reynolds, A. B., Kanner, S. B., Vines, R. R., and Parsons, J. T. (1991) *Mol. Cell. Biol.* **11,** 5113–5124
23. Cary, L. A., Chang, J. F., and Guan, J. L. (1996) *J. Cell Sci.* **109,** (suppl.) 1787–1794
24. Klinghoffer, R. A., Sachsenmaier, C., Cooper, J. A., and Soriano, P. (1999) *EMBO J.* **18,** 2459–2471
25. Zeng, L., Si, X., Yu, W. P., Le, H. T., Ng, K. P., Teng, R. M., Ryan, K., Wang, D. Z., Ponniah, S., and Pallen, C. J. (2003) *J. Cell Biol.* **160,** 137–146
26. Mariotti, A., Kedeshian, P. A., Dans, M., Curatola, A. M., Gagnoux-Palacios, L., and Giancotti, F. G. (2001) *J. Cell Biol.* **155,** 447–458
27. Wary, K. K., Mariotti, A., Zurzolo, C., and Giancotti, F. G. (1998) *Cell* **94,** 625–634
28. Schaller, M. D., Hildebrand, J. D., Shannon, J. D., Fox, J. W., Vines, R. R., and Parsons, J. T. (1994) *Mol. Cell. Biol.* **14,** 1680–1688
29. Giancotti, F. G., and Ruoslahti, E. (1999) *Science* **285,** 1028–1032
30. Schlaepfer, D. D., Broome, M. A., and Hunter, T. (1997) *Mol. Cell. Biol.* **17,** 1702–1713
31. Schlaepfer, D. D., Jones, K. C., and Hunter, T. (1998) *Mol. Cell. Biol.* **18,** 2571–2585
32. Kanner, S. B., Reynolds, A. B., Vines, R. R., and Parsons, J. T. (1990) *Proc. Natl. Acad. Sci. U. S. A.* **87,** 3328–3332
33. Zhan, X., Hu, X., Hampton, B., Burgess, W. H., Friesel, R., and Maciag, T. (1993) *J. Biol. Chem.* **268,** 24427–24431
34. Li, Y., Tondravi, M., Liu, J., Smith, E., Haudenschild, C. C., Kaczmarek, M., and Zhan, X. (2001) *Cancer Res.* **61,** 6906–6911
35. Mitchison, T. J., and Cramer, L. P. (1996) *Cell* **84,** 371–379
36. Schuuring, E. (1995) *Gene (Amst.)* **159,** 83–96
37. Patel, A. S., Schechter, G. L., Wasilenko, W. J., and Somers, K. D. (1998) *Oncogene* **16,** 3227–3232
38. Head, J. A., Jiang, D., Li, M., Zorn, L. J., Schaefer, E. M., Parsons, J. T., and Weed, S. A. (2003) *Mol. Biol. Cell* **14,** 3216–3229

The EMBO Journal (2004) 23, 1075–1088 | © 2004 European Molecular Biology Organization | All Rights Reserved 0261-4189/04
www.embojournal.org

THE EMBO JOURNAL

Tiam1 mediates neurite outgrowth induced by ephrin-B1 and EphA2

Masamitsu Tanaka[1,2], Riuko Ohashi[1,3], Ritsuko Nakamura[1], Kazuya Shinmura[1], Takaharu Kamo[1], Ryuichi Sakai[2] and Haruhiko Sugimura[1,*]

[1]First Department of Pathology, Hamamatsu University School of Medicine, Handayama, Hamamatsu, Japan and [2]Growth Factor Division, National Cancer Center Research Institute, Tsukiji, Chuo-ku, Tokyo, Japan

Bidirectional signals mediated by Eph receptor tyrosine kinases and their membrane-bound ligands, ephrins, play pivotal roles in the formation of neural networks by induction of both collapse and elongation of neurites. However, the downstream molecular modules to deliver these cues are largely unknown. We report here that the interaction of a Rac1-specific guanine nucleotide-exchanging factor, Tiam1, with ephrin-B1 and EphA2 mediates neurite outgrowth. In cells coexpressing Tiam1 and ephrin-B1, Rac1 is activated by the extracellular stimulation of clustered soluble EphB2 receptors. Similarly, soluble ephrin-A1 activates Rac1 in cells coexpressing Tiam1 and EphA2. Cortical neurons from the E14 mouse embryos and neuroblastoma cells significantly extend neurites when placed on surfaces coated with the extracellular domain of EphB2 or ephrin-A1, which were abolished by the forced expression of the dominant-negative mutant of ephrin-B1 or EphA2. Furthermore, the introduction of a dominant-negative form of Tiam1 also inhibits neurite outgrowth induced by the ephrin-B1 and EphA2 signals. These results indicate that Tiam1 is required for neurite outgrowth induced by both ephrin-B1-mediated reverse signaling and EphA2-mediated forward signaling.

The EMBO Journal (2004) **23**, 1075–1088. doi:10.1038/sj.emboj.7600128; Published online 26 February 2004
Subject Categories: signal transduction; cell & tissue architecture
Keywords: cortical neuron; Eph; ephrin; neurite outgrowth; Tiam1

Introduction

The members of the Eph receptors and their ligands are variously involved in neural development: regulating axon guidance, axon fasciculation and synaptogenesis. The interaction of Eph and ephrin regulates axon guidance by a repulsive function. Retinal axons expressing EphA receptors are guided to their target tectal area according to interactions with a repellent ephrin-A gradient (Cheng *et al*, 1995). The pathfinding of mouse anterior commissure is also regulated by the repulsive function between ephrin-B1 and EphB2 receptor (Henkemeyer *et al*, 1996). On the other hand, the interaction of Eph and ephrin also induces attractive axon guidance in certain settings. Vomeronasal axons expressing ephrin-A5 are attractively elongated by interaction with target EphA receptors in the accessory olfactory bulb, implying that ephrin-A mediates attractive guidance mechanisms (Knoll *et al*, 2001). Another example of attractive axon guidance is also reported in terms of the interaction of the EphB receptor and ephrin-B. Mann *et al* (2002) show that *Xenopus* dorsal retinal axons expressing ephrin-B preferentially project to the tectal area where EphB1 is highly expressed, while the ventral ones that express EphB2 project to the dorsal area of the tectum where ephrin-Bs are highly expressed. Therefore, Eph receptors and ephrins are involved in both repulsive and attractive guidance mechanisms during the establishment of neuronal connections. Gao *et al* have previously shown the two opposing effects of Eph receptors and ephrins on neurite outgrowth *in vitro* by a series of experiments. Primary cultured rat neurons extended or retracted neurites when they were plated on cells stably expressing various Eph or ephrins on their surface (Gao *et al*, 1996, 1998, 1999, 2000). However, the molecular basis of such morphological change requires investigation.

Rho GTPases are important regulators of the actin cytoskeleton. Activation of RhoA and its effector protein Rho-kinase (ROCK) leads to growth cone collapse, neurite retraction or neurite growth inhibition by inducing the contraction of actomyosin (Wahl *et al*, 2000). On the other hand, activation of Rac1 induces neurite elongation. Tiam1, a specific guanine-nucleotide exchange factor (GEF) for Rac1 (Habets *et al*, 1994), affects neuronal morphology (Leeuwen *et al*, 1997; Kunda *et al*, 2001). Moreover, STEF, another GEF for Rac1, which has highly homologous regions with Tiam1, is also effective in neurite outgrowth (Matsuo *et al*, 2002). The cellular localization of Tiam1 and EphA2 is similar. When cells were cultured sparsely, both EphA2 and activated Tiam1 are highly expressed at the cell periphery containing membrane ruffles. However, when cells were adhered to each other, they are highly expressed at the site of cell-to-cell adhesion (Sander *et al*, 1998; Zantek *et al*, 1999). These observations led us to focus on the examination whether Tiam1 and EphA2 interact, and Tiam1 could be a mediator of EphA2 receptor. During the examination of the interaction of Tiam1 with several Eph receptors and ephrins, we have found that ephrin-B1 also associates with Tiam1.

In this study, we describe the interaction of Tiam1 with ephrin-B1 and EphA2. A part of Tiam1 was accumulated to the sites including clustered ephrin-B1 and EphA2 after the

*Corresponding author. First Department of Pathology, Hamamatsu University School of Medicine, 1-20-1 Handayama, Hamamatsu 431-3192, Japan. Tel.: +81 53 435 2220; Fax: +81 53 435 2225; E-mail: hsugimur@hama-med.ac.jp
[3]Present address: Division of Cellular and Molecular Pathology, Department of Cellular Function, Niigata University Graduate School of Medical and Dental Sciences, Asahimachi-dori 1, Niigata 951-8510, Japan

Received: 9 April 2003; accepted: 19 January 2004; published online: 26 February 2004

cells were stimulated with EphB2 and ephrin-A1, respectively. Neurite outgrowth was observed in primary cortical neurons from mouse embryos in response to the stimulation of EphB2-Fc, and NB1 neuroblastoma cells in response to ephrin-a1-Fc. Coexpression of the dominant-negative mutant of Tiam1, or mutant of ephrin-B1 or EphA2, which lacks its cytoplasmic region prevented the neurite extension described above. These results suggest that Tiam1 is a mediator of ephrin-B1- and EphA2-induced neurite outgrowth.

Results

Tiam1 interacts with the cytoplasmic domain of ephrin-B1 and EphA2

We have examined the association between Tiam1 with ephrin-B1 and EphA2 *in vivo*. Coexpression and co-precipitation analysis in COS1 cells revealed that Tiam1 was co-precipitated with ephrin-B1 and EphA2 by specific antibodies (Figure 1A, lanes 1 and 3, arrowheads, respectively), but not by the normal goat serum or mouse IgG1 (Figure 1A, lanes 2 and 4, arrowheads, respectively). These results were further confirmed by experiments using the antibodies in reverse order. Ephrin-B1 and EphA2 were co-precipitated with Tiam1 (Figure 1A, lanes 5 and 7, arrowheads, respectively). Next, we have generated several truncated mutants of Tiam1 to determine the region within Tiam1, which is required for the interaction with ephrin-B1 or EphA2 (Figure 1B). Among the truncated mutants of Tiam1, N-terminal-deleted Tiam1 (C1199) tightly bound to ephrin-B1, but Tiam1 encoding 392 amino-terminal amino acids (N392) did not associate with ephrin-B1 (Figure 1C, lanes 1–4). Reciprocally, EphA2 interacted with Tiam1 (N392), but did not associate with Tiam1 (C1199) (Figure 1C, lanes 5–8). These results indicate that ephrin-B1 and EphA2 interact with different regions of Tiam1.

To identify the region of the Tiam1 protein essential for the interaction with ephrin-B1 or EphA2, we performed an *in vitro* glutathione *S*-transferase (GST) fusion protein pull-down assay. *In vitro*-translated Tiam1 was co-precipitated with the GST-tagged cytoplasmic region of ephrin-B1 (ephrin-B1$^{264-346}$) or EphA2 (EphA2$^{563-977}$) but not by the control GST alone (Figure 2, top). The cytoplasmic region of ephrin-B1 did not bind to Tiam1 (N392). As shown in Figure 2 (bottom), ephrin-B1 clearly associated with the PHnTSS region of Tiam1, which is also included in C1199 and N1041. Therefore, we concluded that the cytoplasmic region of ephrin-B1 binds to Tiam1 via its PHnTSS region. The PHnTSS region contains amino-terminal PH domain, which is known to involve in membrane targeting of Tiam1 protein, and TSS domain, which is conserved among Tiam1, STEF and SIF proteins (Matsuo *et al*, 2002). On the other hand, the GST-tagged cytoplasmic region of EphA2 did not associate with the PHnTSS region of Tiam1, but instead associated with Tiam1 constructs harboring the amino-terminal region of Tiam1 (N392). We assume that EphA2 binds to Tiam1 via its amino-terminal region (Tiam1$^{1-392}$). Although the association of Tiam1 with ephrin-B1 was detected without activation of ephrin-B1 by the extracellular domain (ECD) of EphB2, we found that the GST-tagged PHnTSS domain of Tiam1 expressed in 293T cells was co-precipitated with ephrin-B1 more effectively after the incubation with EphB2-Fc (Supplementary information 3A).

Finally, we examined the *in vivo* status of Tiam1 with ephrin-B1/EphA2 in the E14 mouse brain, where Tiam1 and ephrin-B1 are highly expressed. Tiam1 was co-precipitated with ephrin-B1 from an extract of E14 mouse whole brain by the specific antibody, but not by normal goat serum (Figure 3A). Although EphA2 in the whole brain of E14 mouse is expressed at a low level, endogenously expressed Tiam1 protein was co-immunoprecipitated with EphA2 but not with the control mouse IgG1 (Figure 3B). The interaction of ephrin-B1 and EphA2 with Tiam1 in the mouse brain was further confirmed by experiments using the antibodies in reverse order. Ephrin-B1 and EphA2 were co-precipitated with Tiam1 by the specific antibodies, but not by normal rabbit serum (Figure 3C and D). The size of endogenous ephrin-B1 protein in the mouse brain was slightly larger than transiently expressed ephrin-B1 in COS1 cells.

Tiam1 is translocated after stimulation with the extracellular domain of EphB2 or ephrin-A1

Next, we examined the cellular localization of Tiam1, ephrin-B1 and EphA2. Ephrin-B reverse signaling is known to induce the formation of large membrane patches containing several proteins after stimulation with preclustered EphB2-Fc (Cowan and Henkemeyer, 2002; Palmer *et al*, 2002). In SK-N-MC cells, intense staining of endogenous ephrin-B1 protein is observed in the cell membrane at the contact of cell-to-cell adhesion (Figure 4A, column c, top). Concomitantly with the stimulation of EphB2-Fc, patches containing ephrin-B1 were formed mostly in the cell membrane (Figure 4A, column a, top panel). As expected, the colocalization of ephrin-B1 in patches containing EphB2-Fc was also confirmed in SK-N-MC cells (Supplementary information 2, column a). Tiam1 protein is homogenously expressed in the cytoplasm before

Figure 1 Tiam1 forms a complex with ephrin-B1 and EphA2 receptor. (**A**) COS1 cells were transiently transfected with a plasmid encoding wild-type Tiam1 together with that encoding ephrin-B1 (lanes 1, 2, 5, 6) or EphA2 (lanes 3, 4, 7, 8). Cells were lysed and immunoprecipitated (IP) with anti-ephrin-B1 (goat polyclonal, lane 1), normal goat serum (NGS, lane 2), anti-EphA2 (lane 3), mouse IgG1 (lane 4), anti-Tiam1 (lanes 5, 7) or normal rabbit serum (NRS, lanes 6, 8). The precipitates were subjected to immunoblotting (IB) with the indicated antibodies. The same membranes were reblotted with the antibodies indicated (bottom panels). The expression of Tiam1, ephrin-B1 and EphA2 in the cell lysate was confirmed by immunoblotting. When wild-type ephrin-B1 is overexpressed in COS1 cells, at least two major bands were observed by anti-ephrin-B1 goat polyclonal antibody. Ig, immunoglobulin. The prominent band of 80 kDa in lane 3 is an unknown protein, which associates with EphA2 and may have a related structure with Tiam1. (**B**) Schematic representation of a wild-type and the truncated Tiam1 cDNA constructs used in this study. Proteins are depicted to scale; M, myristoylation signal; PHn and PHc, NH2- and COOH-terminal pleckstrin homology domains; TSS, otherwise known as coiled-coil region and an additional adjacent region (CC-Ex); PDZ, PSD-95/DlgA/ZO-1 domain; DH, Dbl homology domain. (**C**) COS1 cells were transiently transfected with the plasmids as indicated in the above lanes. The cell lysates were immunoprecipitated with anti-ephrin-B1 C18 (lanes 1, 3), EphA2 (lanes 5, 7), normal rabbit serum (lanes 2, 4) or mouse IgG1 (lanes 6, 8) and immunoblotted with anti-myc antibody. The same membranes were reblotted with anti-ephrin-B1 (goat) or anti-EphA2 as indicated. The expression of myc-tagged Tiam1 constructs in these cell lysates (total lysate) was confirmed by immunoblotting. The additional band at 110 kDa in lane 1 may be an artificially produced fragment of overexpressed Tiam1 construct.

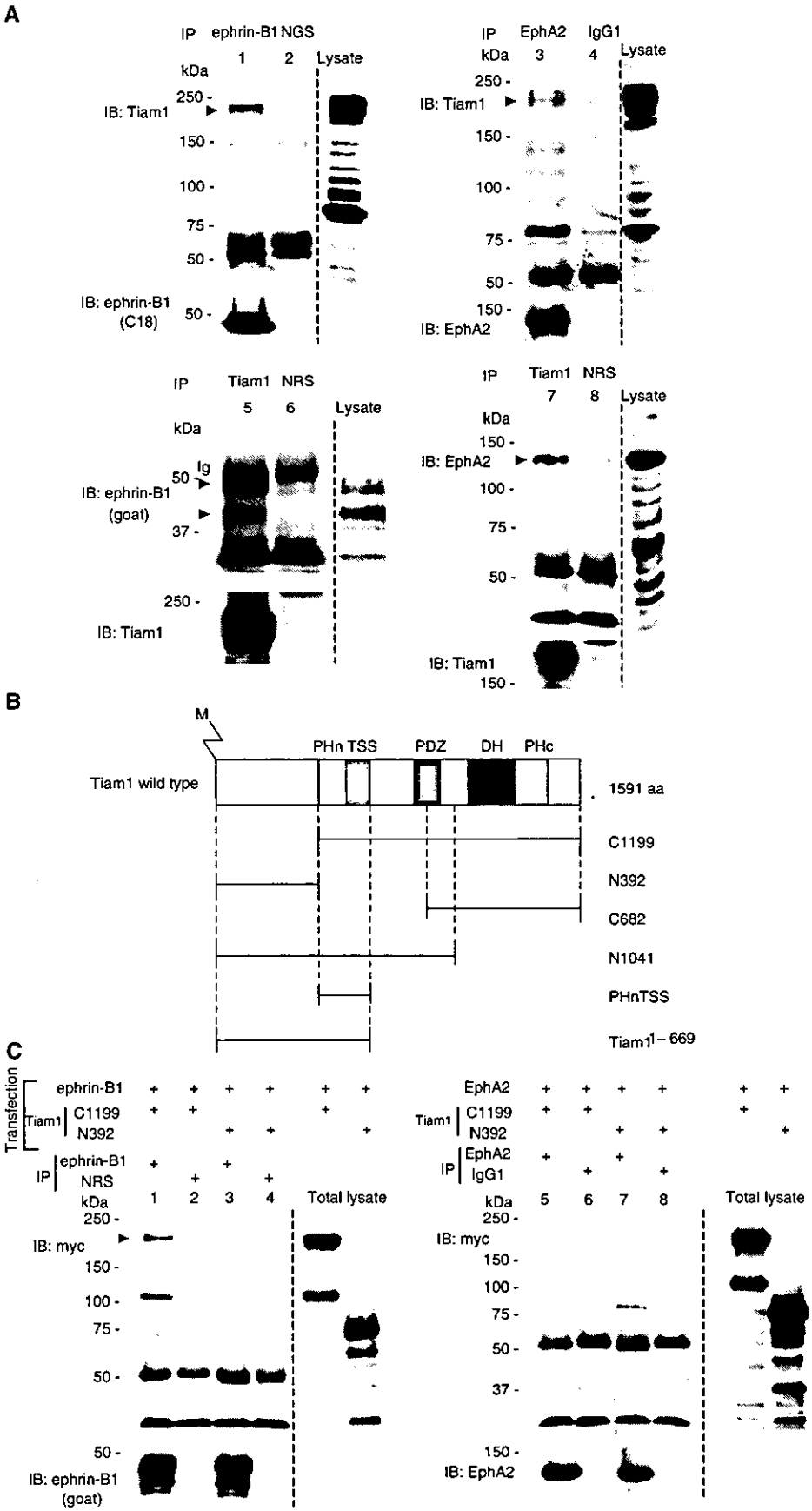

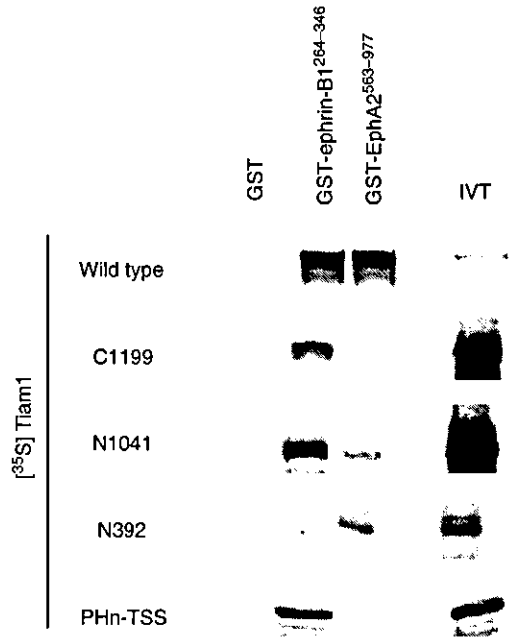

Figure 2 Tiam1 binds to ephrin-B1 and EphA2 *in vitro*: [^{35}S]methionine -labeled wild type or truncated mutants of Tiam1 (C1199, N1041, N392, PHnTSS) translated products were incubated with glutathione–agarose-conjugated GST, GST-ephrin-B1$^{264-346}$ and GST-EphA2$^{563-977}$, respectively. IVT, the input of *in vitro* translation reaction before the beads binding.

stimulation with EphB2-Fc (Figure 4A, column c, middle). However, at least a part of Tiam1 was clearly found to colocalize to the patches after exposure to preclustered EphB2-Fc (Figure 4A, column a, middle and bottom). Although there were a few spotty stains of both ephrin-B1 and Tiam1 in the cells without stimulation of EphB2-Fc, they never colocalized as shown in the merged panel (Figure 4A, column c). In order to exclude the possibility that the second antibodies used directly recognize the clustered Fc fusion proteins, we have shown that there is almost no staining of Tiam1 protein by staining with the secondary antibody without prior incubation with the primary anti-Tiam1 antibody (Figure 4A, column b). We also confirmed that the preincubation of anti-Tiam1 antibody with the blocking peptide (Tiam1 C16) or the bacterially produced GST fusion protein of Tiam1$^{1430-1591}$ containing its C-terminal region abolished Tiam1 staining (data not shown). In the primary cortical neurons from E14 mouse embryos, ephrin-B1 is highly expressed on the cell membrane and neurites, and Tiam1 protein is distributed in the cytoplasm of the cell body and neurites (Figure 4B, columns c and d). Tiam1 and ephrin-B1 were also copatched in E14 cortical neurons 1 h after stimulation with clustered EphB2-Fc (Figure 4B, columns a and b). We observe many patches containing Tiam1 and ephrin-B1 on the elongated neurites and the periphery of cell bodies of these neurons, while there was no such patchy localization of Tiam1 in the neurons without stimulation with EphB2-Fc. In Supplementary information 2, we show the precise colocalization of ephrin-B1 with EphB2-Fc patches, and that in the control there was no crossreaction of the rhodamine-labeled secondary antibody to clustered Fc fusion protein in primary cortical neurons (columns b and c, respectively).

NB1 neuroblastoma cells express EphA2 and Tiam1 endogenously as described later. Before stimulation of NB1 cells with ephrin-A1-Fc, there was no patchy localization of EphA2 detected by immunostaining. Intense staining of EphA2 was located on the cell membrane, especially at the sites of cell-to-cell contact (Figure 4C, column c, top). In the same manner as is the case with cortical neurons, Tiam1, initially distributed homogenously in the cytoplasm (Figure 4C, column c, middle), was partly translocated to patches containing EphA2 after stimulation with soluble ephrin-A1 (Figure 4C, column a, middle and bottom). The patches containing EphA2 localized not only on the cell membrane but also in the cytoplasm, which may be a consequence of the internalization of EphA2 from the cell membrane after stimulation of its ligand. Such internalization of ligand-stimulated EphA2, and more recently ephrin-B1, has been reported (Walker-Daniels *et al*., 2002; Zimmer *et al*., 2003). There was no crossreaction of the secondary antibody to the clustered ephrin-A1-Fc protein (Figure 4C, column b). These results together demonstrate the colocalization of Tiam1 with ephrin-B1 and EphA2, and the distribution of Tiam1 is at least partly translocated after stimulation of ephrin-B1 and EphA2.

Tiam1 is involved in Rac1 activation induced by Eph/ephrin signaling

To analyze whether Eph/ephrin signaling mediates Tiam1 activation, we examined the modification of Tiam1-induced Rac1 activation by the affinity precipitation of GTP-bound Rac1 with the GST-tagged p21-binding domain of PAK1 (GST-PBD). Rac1 was slightly activated by the overexpression of wild-type Tiam1 (Figure 5A, compare lanes 1 and 2). Although Rac1 was also slightly activated after stimulation with EphB2-Fc in ephrin-B1-expressing cells (Figure 5A, lane 3), the amount of GTP-bound Rac1 was markedly increased in response to the stimulation by EphB2-Fc when both Tiam1 and ephrin-B1 are expressed (Figure 5A, compare lanes 4 and 5). Because the PHnTSS region of Tiam1 works as a dominant-negative mutant of Tiam1 (Stam *et al*, 1997), we next examined whether PHnTSS of Tiam1 blocks the Rac1 activity induced by the activation of ephrin-B1. The activation of Rac1 induced by the stimulation of EphB2-Fc was completely abolished by the coexpression of PHnTSS of Tiam1, but not by the coexpression of Tiam1 (N392) (Figure 5A, lanes 8 and 9). The coexpression of EphA2 and Tiam1 did not induce Rac1 activation significantly without stimulation of ephrin-A1-Fc (Figure 5A, lane 10). The overexpression of EphA2 alone is not effective in activating Rac1 even though the cells were stimulated by ephrin-A1 (Figure 5A, lane 15). The stimulation of ephrin-A1-Fc activated Rac1 in cells expressing EphA2 and Tiam1, which was blocked by the coexpression of Tiam1$^{1-669}$ (Figure 5A, compare lanes 11 and 12). The coexpression of PHnTSS partly inhibited the ephrin-A1-Fc-induced Rac1 activation, and Tiam1$^{1-392}$ blocked the Rac1 activation very effectively but not completely (Figure 5A, lanes 13 and 14).

We next examined the phosphorylation of Tiam1 by the activation of ephrin-B1 or EphA2. When ephrin-B1-expressing cells were cocultured with cells expressing kinase-inactivated EphB2 (EphB2K661M), ephrin-B1 was highly phosphorylated on tyrosine residues, but not when cocultured with control mock-transfected cells as we have described before (Figure 5B, lanes 1 and 2, bottom) (Tanaka *et al*, 2003). Similarly, the tyrosine phosphorylation of EphA2 was in-

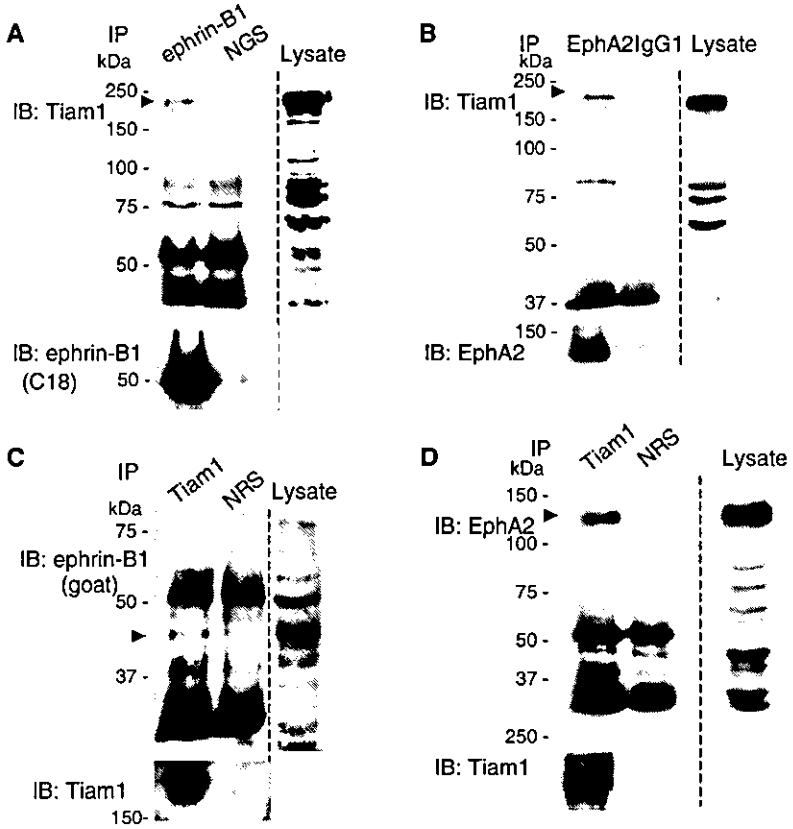

Figure 3 Tiam1 physiologically interacts with ephrin-B1 and EphA2 in the brain of an E14 mouse embryo. Whole brains from E14 mice embryos were lysed and immunoprecipitated (IP) with anti-ephrin-B1 (goat), anti-EphA2, anti-Tiam1, normal goat serum (NGS), normal rabbit serum (NRS) or mouse IgG1 respectively as indicated in the above lanes. The precipitates were subjected to immunoblotting (IB) with the indicated antibodies. Co-precipitated Tiam1, ephrin-B1 and EphA2 are indicated by arrowheads. In (C), the upper band of ephrin-B1 was overlapped with the band of immunoglobulin. The membranes were reblotted with antibodies indicated (bottom panels).

creased when EphA2-expressing cells were cocultured with cells expressing ephrin-A1 (Figure 5B, lanes 5 and 6, bottom). The activation of ephrin-B1 by overlaying the EphB2-expressing cells leads to weak phosphorylation of Tiam1 as detected by labeling cells with orthophosphate (Figure 5B, lanes 1 and 2). Tiam1 is also phosphorylated upon stimulation of EphA2 by coculturing with cells expressing ephrin-A1 (Figure 5B, lanes 3 and 4). Moreover, Tiam1 is phosphorylated on tyrosine residues by the stimulation of EphA2-mediated signaling, as detected by immunoblotting with anti-phosphotyrosine antibody (Figure 5B, lanes 5 and 6). On the other hand, we did not clearly detect phosphorylation of Tiam1 in response to activation of ephrin-B1 on either tyrosine residues (examined by the same method as above) or on serine/threonine residues by immunoblotting with the antibodies described in Supplementary information 1 (data not shown).

Neurite outgrowth by ephrin-B1–Tiam1 and EphA2–Tiam1 interaction

We first confirmed that the dissociated primary cultured cells of E14 cortical neurons still maintain the expression of Tiam1, ephrin-B1, EphB2 and EphA4 *in vitro*, although the expression levels of these proteins were higher in the cortical tissue compared to dissociated cortical cells (Figure 6E). When E14 cortical neurons were seeded on preclustered EphB2-Fc-coated plates, ephrin-B1 is phosphorylated on tyrosine residues at 30 min and 4 h after plating (Figure 6E, bottom). Around 31% of the cells seeded on EphB2-Fc-coated plates show neurites longer than one cell body in length (Figure 6A, Table I), which is statistically different from the numbers when plated on the clustered Fc only or on the albumin (Figure 6B and C). The effect of ephrin-A1-Fc on neurite outgrowth of E14 mouse cortical neurons was weaker than the stimulation of EphB2-Fc (Figure 6D, Table I). In particular, the number of cells bearing longer neurites (longer than three cell bodies in length) was much smaller when cells were seeded on ephrin-A1-Fc-coated plates than on EphB2-Fc-coated plates (Table I). EphA2 expression in the cortex of E14-16 was monitored in brain lysates, because we suspect that the weak expression in this area and the developmental stage may be one of the reasons for the less dramatic effect on neurite outgrowth. Actually, the expression of EphA2 was barely detectable in the cortex region of this stage (Figure 6E), while it was detectable in the whole brain lysate (Figure 3). We did not observe any elongated neurites on ephrin-B1-Fc-coated plates (data not shown).

In the neuroblastoma cell line NB1, a considerable expression of Tiam1 and EphA2 was detected (Figure 7D). We also confirmed that NB1 cells do not express detectable level of EphA4 (Figure 7D). We used this NB1 system in the following experiments for evaluation of EphA2 forward signaling. The

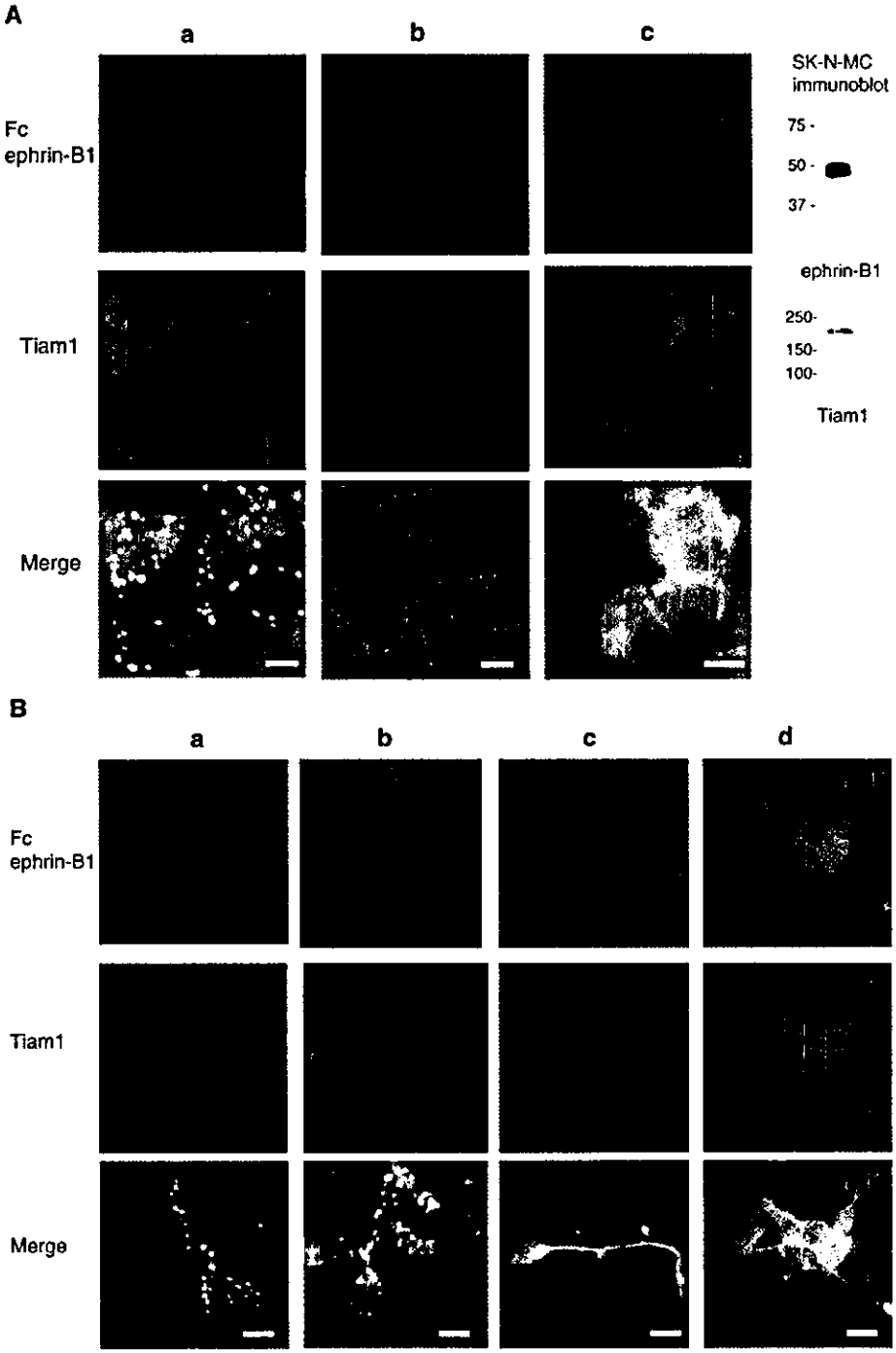

Figure 4 Tiam1 is recruited to patches induced by EphB2-Fc- or ephrin-A1-Fc stimulation. (**A**) SK-N-MC cells expressing ephrin-B1 were stimulated with 4 μg/ml of clustered EphB2-Fc (columns a, b) or left untreated (column c). After 10 min of stimulation, the cells were washed and incubated in a medium without EphB2-Fc for 1 h prior to fixation. The cells were immunostained with anti-Fc (green) and anti-Tiam1 (red) antibodies (column a). In column b, incubation with primary anti-Tiam1 antibody was omitted prior to incubation with the rhodamine-labeled secondary antibody. Column c shows the signals with anti-ephrin-B1 staining (green) and anti-Tiam1 staining (red). Expressions of Tiam1 and ephrin-B1 in SK-N-MC cells are shown by immunoblot. (**B**) (Columns a, b) E14 mouse cortical neurons were cultured for 20 h on poly-L-lysine-coated slides, and then stimulated with EphB2-Fc for 1 h as described above. The cells were fixed and immunostained with anti-Fc (green) and anti-Tiam1 (red) antibodies. (Columns c, d) Localization of ephrin-B1 (green) and Tiam1 protein (red) without stimulation of EphB2-Fc is shown. (**C**) (Columns a, b) NB1 neuroblastoma cells were stimulated with 4 μg/ml of clustered ephrin-A1-Fc as described in (A). The cells were immunostained with anti-Fc (green) and anti-Tiam1 (red) antibodies. In column b, incubation with primary anti-Tiam1 antibody was omitted prior to incubation with the rhodamine-labeled secondary antibody. (Column c) Localization of EphA2 (green) or Tiam1 protein (red) without stimulation of ephrin-A1-Fc is shown. Scale bar, 10 μm.

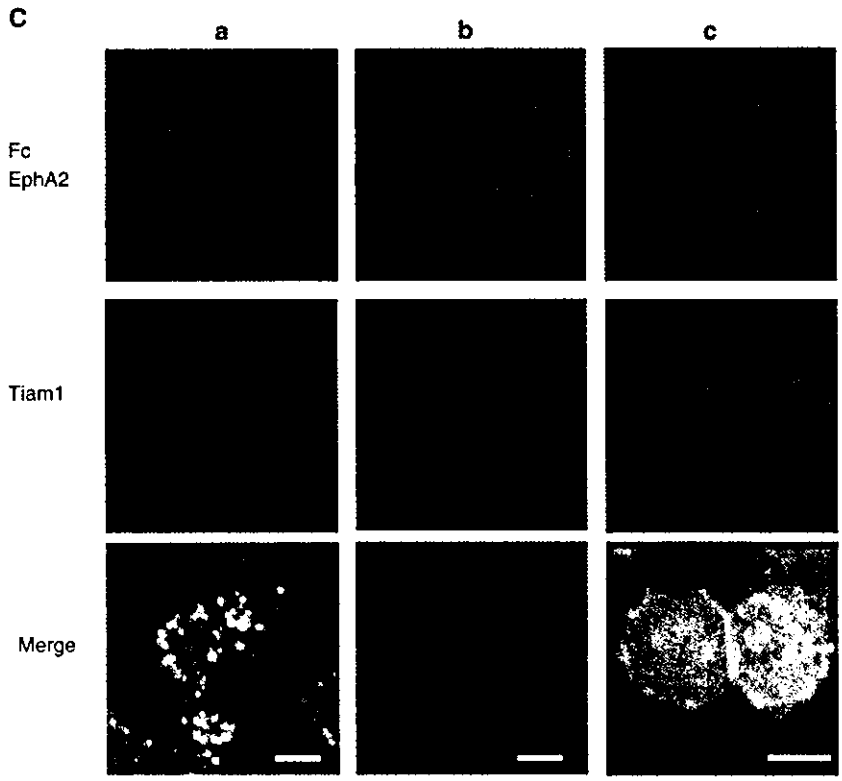

Figure 4 (Continued)

tyrosine phosphorylation of EphA2 was clearly demonstrated at 30 min and 4 h after plating on ephrin-A1-Fc-coated dish (Figure 7D, bottom). The decreased expression level of EphA2 after stimulation is considered to be a result of negative regulation of activated EphA2 by Cbl-mediated ubiquitination (Wang *et al*, 2002). When NB1 cells were plated on a surface coated with preclustered ephrin-A1-Fc, many cells exhibited long thin neurites after 16 h of incubation (Figure 7B), whereas few cells bearing such neurites were observed in cells plated on the control Fc-coated plates (Figure 7A). The elongated neurites were not observed on preclustered EphA2-Fc-coated plate, either, as shown in Figure 7C.

To confirm that the outgrowth of neurites observed above depends on the interaction of EphB2 or ephrin-A1 with its cognate ligand or receptor, we did several experiments interfering with this pathway by a soluble ligand or receptor and a dominant-negative or defective competitor in the following experiments. When the cells were plated on Fc fusion protein-coated surface as above with an excess volume of the soluble ephrin-B1-Fc or EphA2-Fc in the medium, the neurite outgrowth of E14 cortical neurons plated on the EphB2-Fc surface and neurite outgrowth of NB1 cells plated on the ephrin-A1-Fc surface were blocked, respectively. However, the addition of soluble ephrin-B1 or EphA2 in the medium had no effect on the nonspecific neurite outgrowth of E14 cortical neurons and NB1 cells induced by plating cells on a poly-L-lysine-coated surface (data not shown). Furthermore, the forced expression of an ephrin-B1 mutant lacking its cytoplasmic region (ephrin-B1$^{1-265}$) in E14 mouse cortical neurons lessened the effect both in numbers and length of neurites, while the expression of control EGFP did not affect the neurite outgrowth (Figure 8, compare A and B). Likewise, the expression of mutants of EphA2 lacking its cytoplasmic region (EphA2$^{1-540}$) in neuroblastoma cells reduced the number of these cells bearing neurites on an ephrin-A1-coated surface (Figure 8, compare E and F).

Finally, we examined whether dominant-negative mutants of Tiam1 inhibit the neurite outgrowth induced by the ephrin-B1- or EphA2-mediated signaling. E14 cortical neurons on the EphB2-Fc surface were transiently transfected with the PHnTSS region of Tiam1 tagged with EGFP. On the other hand, we used Tiam1$^{1-669}$ to test whether it could block the neurite outgrowth induced by EphA2-mediated signaling, because it effectively blocked the Rac1 activation induced by the activation of EphA2 (Figure 5A). As shown in Figure 8C, the neurite outgrowth of cortical neurons on the EphB2-Fc surface was significantly inhibited by the expression of PHnTSS protein. Similarly, NB1 cells expressing Tiam1$^{1-669}$ did not show apparent neurites on the ephrin-A1-Fc-coated surface (Figure 8G). On the other hand, the expression of these Tiam1 fragments did not effectively inhibit the nonspecific neurite outgrowth of cortical neurons and NB1 cells induced by plating the cells on poly-L-lysine-coated plates (data not shown). Moreover, the inhibitory effect of PHnTSS protein on the neurite outgrowth of NB1 cells on the ephrin-A1-Fc-coated surface was modest, and we did not observe any inhibition of neurite outgrowth by Tiam1$^{1-392}$ in cortical neurons on the EphB2-Fc-coated surface (data not shown). Taken together, these results (Figure 8D and H)

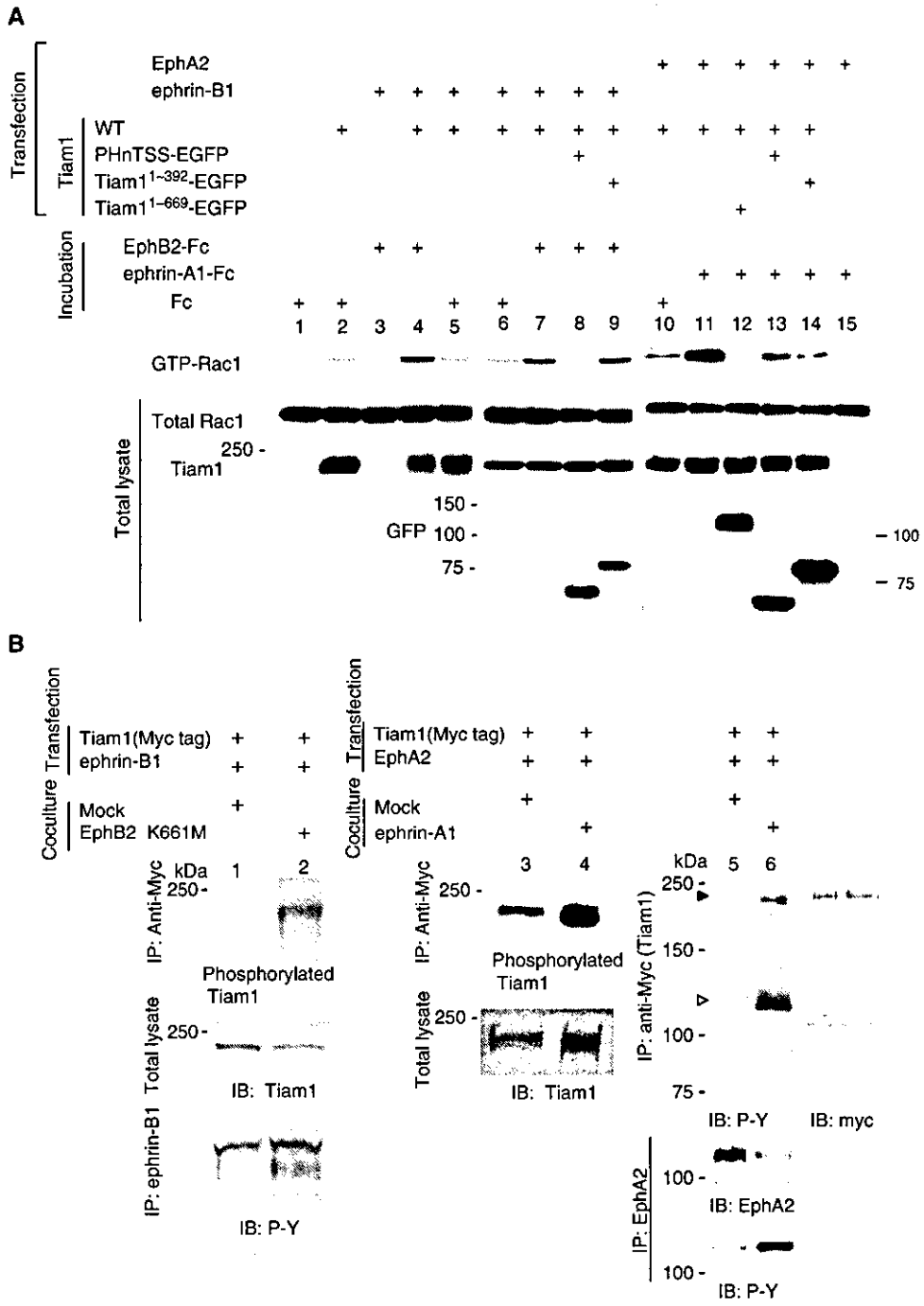

Figure 5 Tiam1 mediates Eph/ephrin-mediated signaling cascades leading to Rac1 activation. (**A**) COS1 cells were transiently transfected with 2 μg of a plasmid encoding wild-type Rac1, together with plasmids indicated in the above lanes. Mock plasmid was used to adjust the amount of DNA to total 10 μg for each transfection. The transfected cells were incubated in media containing clustered EphB2-Fc, ephrin-A1-Fc or control Fc each at a concentration of 5 μg/ml as indicated above the lanes for 15 min before harvesting the cell lysates for affinity precipitation with immobilized GST-PBD. Precipitated GTP-bound Rac1 was detected by immunoblotting with anti-Rac1 antibody. Expression of total Rac1 and Tiam1 is shown at the bottom. (**B**) Phosphorylation of Tiam1 induced by the activation of ephrin-B1 or EphA2 *in vivo*. 293T cells transfected with the plasmids indicated at the top were cocultured with the 293T cells (lane 1), the 293T cells stably expressing EphB2 K661M (lane 2), the NIH3T3 cells (lanes 3, 5) or the NIH3T3 cells stably expressing ephrin-A1 (lanes 4, 6). Lanes 1–4: The coculture was performed in media containing $^{32}P_i$ for 4 h, and then the cells were lysed for immunoprecipitation with anti-myc, separated by SDS–PAGE and visualized by autoradiography. Lanes 1, 2 bottom: The lysates for immunoprecipitation were prepared from the cells as described above except for the labeling with $^{32}P_i$. Lanes 5, 6: The coculture was performed for 30 min before cell lysates were immunoprecipitated with anti-myc and immunoblotted with anti-phospho-tyrosine antibody (4G10). The phosphorylation of Tiam1 is indicated by filled triangle. Co-precipitated EphA2 is indicated by open triangle. The same membrane was reblotted with anti-myc antibody (right panel). The phosphorylation of ephrin-B1 and EphA2 on tyrosine residues is shown at the bottom of lanes 1, 2 and lanes 5, 6, respectively.

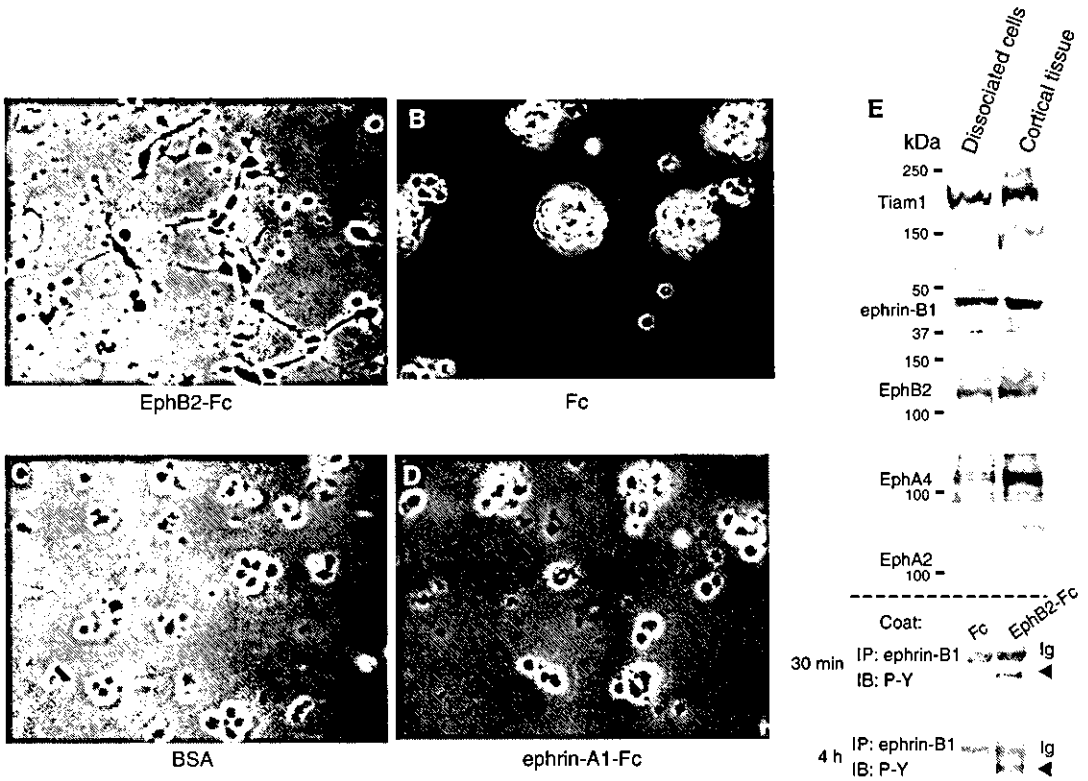

Figure 6 EphB2-Fc induces neurite outgrowth of E14 mouse cortical neurons. Primary cultured cortical neurons from E14 mouse cerebral cortex were seeded on plates coated with EphB2-Fc (**A**), Fc fragment (**B**), bovine serum albumin (BSA) (**C**) or ephrin-A1-Fc (**D**), as described in Materials and methods (Neurite elongation assay). Representative pictures are shown after incubation for 20 h (A–D). (**E**) Expression of Tiam1, ephrin-B1 and various Eph receptors in dissociated primary cultured cells after 20 h incubation on poly-L-lysine-coated dishes, or in the cortical tissues was monitored by immunoblotting. (E, bottom) E14 primary precursors plated on an EphB2-Fc-coated dish were lysed for the indicated period, and immunoprecipitated with anti-ephrin-B1. Tyrosine phosphorylation of ephrin-B1 is shown by immunoblotting.

Table I Quantification of the effects of EphB2-Fc and ephrin-A1-Fc on neurite formation

	Three cell bodies/ total counted[a]	One cell body/total counted[a]
E14 primary cortical neuron[b]		
Fc	0/527 (0%)	0/527 (0%)
BSA	0/531 (0%)	31/531 (5.8%)
EphB2-Fc	61/552 (11.1%)	173/552 (31.3%)
ephrin-A1-Fc	10/523 (1.95)	99/523 (18.9%)
NB1 neuroblastoma cell line[c]		
Fc		0/323 (0%)
ephrin-A1-Fc		115/349 (33.0%)
EphA2-Fc		14/304 (4.6%)

[a]The number of cells possessing neuritis three cell bodies or one cell body was counted 20 h after plating the cells.
[b]Total number of cells counted in four independent experiments.
[c]Total number of cells counted in three independent experiments.

indicate that Tiam1 locates downstream of ephrin-B1- or EphA2-mediated signaling and is involved in the neurite outgrowth.

Discussion

Examination of the association between Tiam1 with ephrin-B1 and EphA2 receptor revealed that Tiam1 interacts with ephrin-B1 and EphA2. Interaction of Tiam1 with EphA2 was not apparently modified by the phosphorylation status of EphA2, because EphA2 with a mutation in its kinase domain and an abolished catalytic activity also associated with Tiam1 as well as wild-type EphA2 (data not shown). However, we cannot completely exclude the possibility that the association of Tiam1 with ephrin-B1 is increased by the stimulation of EphB2-Fc (Supplementary information 3A). The observations that staining of Tiam1 in the cytoplasm did not appear to diminish in the stimulated cells (Figure 4) reveal that only a part of Tiam1 protein translocated to the patches colocalizing with ephrin-B1 or EphA2. Therefore, the localized activation of Tiam1 and Rac1 should be monitored spatially and temporally in these cells in order to evaluate the significance of the translocation of Tiam1. In primary cultured cortical neurons, patches containing ephrin-B1 and Tiam1 often locate along the extended neurites. The biological significance of such colocalization along the neurites requires elucidation. Although Tiam1 is clearly phosphorylated on tyrosine residues by EphA2 activation, we detected phosphorylation of Tiam1 in ephrin-B1-activated cells at low level only by the orthophosphate labeling (Figure 5B). Because the phosphorylation of Tiam1 on threonine residues has been detected by the same antibody in response to the stimulation of platelet-derived growth factor, Tiam1 was not phosphorylated at least on the same positions by the activation of ephrin-B1 (Fleming *et al*, 1998). The significance of the

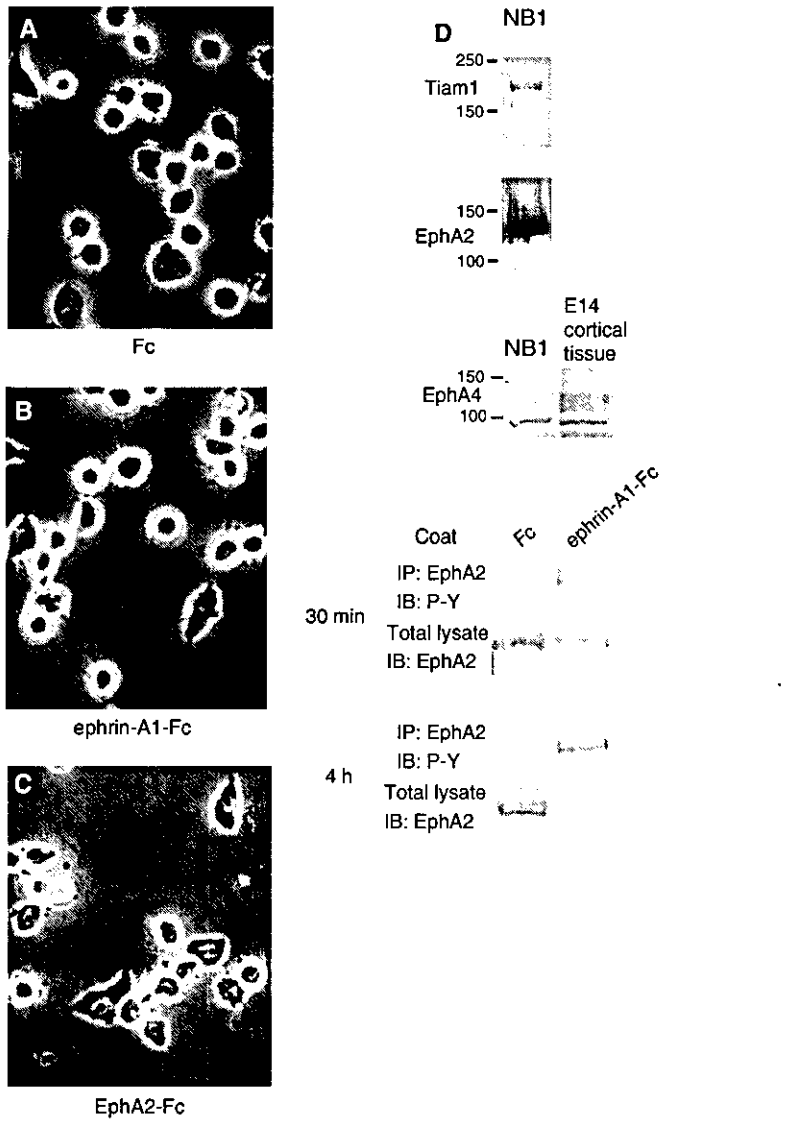

Figure 7 Ephrin-A1-Fc induces neurite outgrowth of NB1 neuroblastoma cells. NB1 neuroblastoma cells were seeded on plates coated with Fc fragment (**A**), ephrin-A1-Fc (**B**) or EphA2-Fc (**C**) as described in Materials and methods. Representative cells are shown after incubation for 20 h (A–C). (**D**) Expression of Tiam1 and Eph receptors in NB1 cells is shown by immunoblotting. (D, bottom) The NB1 cells plated on ephrin-A1-Fc-coated dishes were lysed for the indicated period, and immunoprecipitated with anti-EphA2. Tyrosine phosphorylation of EphA2 is shown by immunoblotting.

phosphorylation of Tiam1 induced by the activation of ephrin-B1 and EphA2 remains to be further studied.

Among proteins reported to be putatively associated with the cytoplasmic regions of Ephs or ephrins, Ephexin, which is a GEF for the rho family GTPases, preferentially interacts with EphA receptors (Shamah *et al*, 2001). Stimulation of ephrin-A regulates growth cone collapse or retraction through Ephexin. Although A-class ephrins are not highly expressed in the developing mouse cortex (Yun *et al*, 2003), it is important to examine the expression of Tiam1 and Ephexin, two exchange factors having opposing effects on the neurites motility, in the cortical region. Furthermore, we also have to consider a homologous protein of Tiam1, STEF, another GEF for Rac1, because STEF is also expressed in the cerebral cortex of developing mice (Matsuo *et al*, 2002; Kawauchi *et al*, 2003). We detected the association of the PHnTSS domain

Figure 8 Expression of dominant-negative mutants of ephrin-B1, EphA2 and Tiam1 affects EphB2-Fc- or ephrin-A1-Fc-induced neurite outgrowth. Primary cultured cortical neurons from E14 mouse embryos (**A–D**), or NB1 cells (**E–H**) were transfected with plasmids encoding either EGFP, EGFP-tagged mutants of ephrin-B1 or EphA2, which lack the cytoplasmic regions (ephrin-B1$^{1-265}$-EGFP, EphA2$^{1-563}$-EGFP), or EGFP-tagged fragments of Tiam1 (PHnTSS-EGFP or Tiam1$^{1-669}$-EGFP). The transfected cells were fixed after 20 h of incubation on slides coated with either EphB2-Fc (A–D) or ephrin-A1-Fc (E–H), and observed through a fluorescence microscope. Representative cells are shown (A–C, E–G). (D, H) Percentage of transfected cells bearing neurites longer than one cell body. Exogenously expressed proteins in these cells were monitored by immunoblotting.

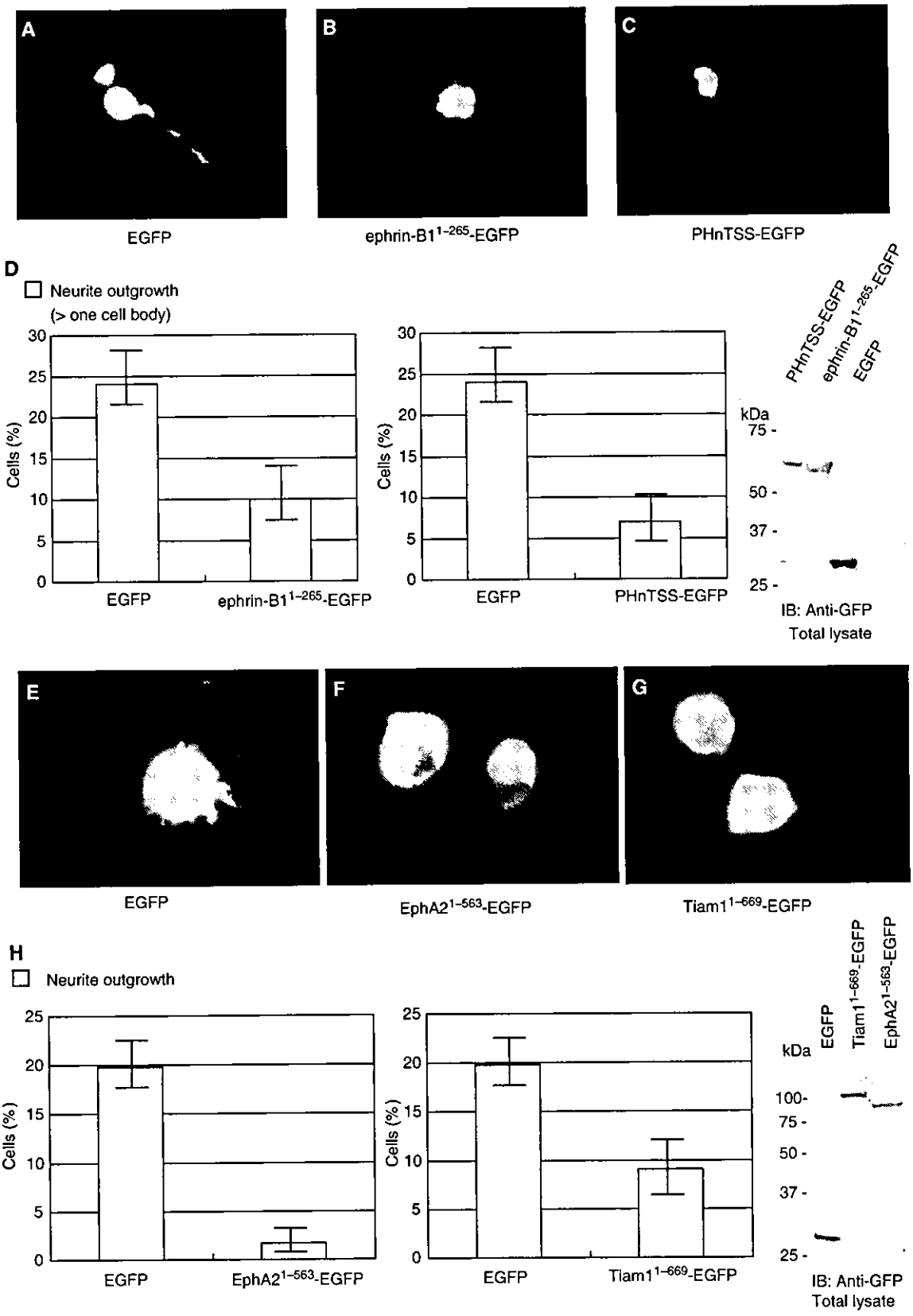

of STEF with ephrin-B1 by immunoprecipitation analysis (Supplementary information 3B). Therefore, the neurite outgrowth may be regulated by exchange factors other than or in addition to Tiam1 in a certain region and stage. In this report, we have used Tiam1 fragments containing the PHnTSS region ($Tiam1^{431-669}$ and $Tiam1^{1-669}$) to block wild-type Tiam1. Because the PHnTSS region of Tiam1 is highly homologous to the PHnTSS domain of STEF, these Tiam1 fragments may also work as dominant-negative mutants for STEF. In addition, we cannot exclude the possibility that Tiam1 fragments containing PHnTSS might antagonize the binding of ephrin-B1 or EphA2 to Tiam1 in addition to acting as a dominant-negative for Tiam1.

The molecular mechanism of the activation of Tiam1 in ephrin-B1- and EphA2-mediated signaling is not clear. Although PHnTSS region is not involved in the association of Tiam1 with EphA2, the expression of PHnTSS inhibited EphA2-induced Rac1 activation mildly, but evidently (Figure 5A). This result may suggest the possibility that EphA2 also activates Tiam1 by a mechanism independent of their association. EphA2 interacts with the p85 subunit of phosphatidylinositol-3-kinase (PI3-kinase) and induces the activation of PI3-kinase (Pandey *et al*, 1994). On the other hand, Tiam1 has been reported to activate by the lipid products of PI3-kinase *in vitro* (Fleming *et al*, 2000). Because PHn (amino-terminal PH domain) is required for the membrane localization and the binding of Tiam1 to the lipid products of PI3-kinase (Stam *et al*, 1997), the overexpression of PHnTSS is considered to block PI3-kinase-dependent Tiam1 activation. Therefore, the inhibitory effect by N392-PHnTSS ($Tiam1^{1-669}$) on the neurite outgrowth of NB1 cells may include a mechanism that may not depend on the association of Tiam1 with EphA2 (Figure 8). However, as shown in Figure 5A, overexpression of N392 alone abolished the Rac1 activation more effectively than PHnTSS. Therefore, the significance of the PI3-kinase for the activation of Tiam1 in EphA2-mediated signaling should be further elucidated.

Concerning the ephrin-B1-mediated reverse signaling on retinal axon growth, both repulsive and attractive guidance has been previously suggested. Birgbauer *et al* (2001) have shown that the ECD of EphB receptors as soluble proteins induced growth cone collapse of ephrin-B-expressing retinal ganglion cells. They also show that axon outgrowth of ephrin-B-expressing dorsal retina explants of E14 mouse was inhibited on the laminin substratum containing EphB-ECD. On the other hand, Mann *et al* (2002) propose an attractive axon guidance that requires the ephrin-B cytoplasmic domain. Retinal axons of *Xenopus* expressing ephrin-Bs prefer to grow on laminin substratum containing EphB receptor stripes *in vitro*. These apparently inconsistent observations may be due to the differences in the experimental procedures, and not to those in the species used between these reports. EphB-Fc protein was used as a dimer in the former (Birgbauer *et al*, 2001) and as a multimer by preclustering with immunoglobulin in the latter (Mann *et al*, 2002); the concentration of laminin substratum used in these reports was also different. In the present study, we followed a procedure similar to that of Mann *et al*, and devised a simplified system for evaluating the outputs of Eph/ephrin-induced signaling. We found that ephrin-B1-expressing cortical neurons markedly extend neurites on surfaces coated with preclustered EphB2-Fc without any other substratum. As to the laminin concentration, the substratum we used contained no laminin, more similar to that used by Mann *et al* (1 μg/ml) than that used by Birgbauer *et al* (10 μg/ml). The lower concentration of laminin seems to prefer the more attractive or progrowth reaction of these systems.

Cell adhesion itself may promote neurite growth, and there are reports concerning adhesive interactions between ephrin-B-expressing axons and the substrate-bound Eph receptor (Holash *et al*, 1997). We also noticed faster attachment of dissociated E14 cortical neurons on EphB2-Fc-coated plates compared to that on Fc-coated plate. We have not directly examined whether Tiam1 mediates this cell-to-substrate adhesion of the cortical neurons, but the adhesion of cortical neurons on the EphB2-Fc surface was accompanied by the phosphorylation of the tyrosine residues of $p130^{Cas}$ and focal adhesion kinase (Supplementary information 4). The primary cultured cortical neurons of E14 mouse embryos adhered to the plates to almost the same degree as a few hours after plating and thereafter, irrespective of whether plates were coated with preclustered-EphB2-Fc, -ephrin-A1-Fc or bovine serum albumin (BSA). Similarly, NB1 cells adhered almost equally to plates precoated with Fc, ephrin-A1-Fc or EphA2-Fc after a few hours of seeding and thereafter. However, we cannot completely exclude the possibility that the differences in neurite outgrowth could depend on differential adhesiveness of the substrates.

Among other members of Eph receptors and ephrins, considerable expression of ephrin-B2 and ephrin-B3 mRNAs is also present in the cortical neurons (Stuckmann *et al*, 2001). Moreover, EphA4 protein is broadly expressed within the cortex of E14 and E16 mouse (Liebl *et al*, 2003; Yun *et al*, 2003). Because the amino-terminal region of Tiam1 ($Tiam1^{1-392}$) also associates with EphA4 leading to the phosphorylation of Tiam1 on tyrosine residues (data not shown), EphA4 receptor may also regulate Rac1 activation by interaction with Tiam1. Further studies are necessary to examine whether Tiam1 also regulates signals mediated by ephrin-B2, ephrin-B3 and EphA4 in the neurons, which may position Tiam1 as a general mediator of Eph/ephrin signals. In NB1 cells, we cannot exclude the possibility that neurite outgrowth of NB1 cells was not exclusively mediated by EphA2.

Our results suggest the importance of Tiam1 and Rac1 as downstream molecules in ephrin-B1- or EphA2-mediated signaling in neurite outgrowth. According to previous information, Eph receptors/ephrins signals, both forward and reverse, have exhibited various, sometimes paradoxical effects on the regulation of neurite extension, that is, retraction and elongation. Our discovery of the involvement of Tiam1 downstream with both the forward and reverse signals of Eph/ephrin system in these neurite responses provides insight that the selection of the GEFs actually working downstream to Ephs/ephrins may determine the fate of neurites.

Materials and methods

Plasmids and antibodies

Plasmids and antibodies used in these series of experiments are described in Supplementary information 1.

Cell culture and transfection

SK-N-MC neuroepithelioma cells and NB1 neuroblastoma cells were cultured in RPMI 1640 supplemented with 10% fetal bovine serum.

The cerebral cortex from E14 DDY mouse embryos were dissected, dissociated and plated on chamber slides as described (Ueki *et al*, 1993), and cultured in DMEM supplemented with D-glucose (4.5 g/l) and 10% fetal bovine serum. For transient expression assays, NB1 cells were transfected with plasmid DNA using Lipofectamine 2000 (GIBCO-BRL), and 293T cells and COS1 cells were transfected with plasmid DNA either by a calcium phosphate co-precipitation method essentially as described previously (Otsuki *et al*, 2001) or using FuGENE6 reagent (Roche). For the transfection of plasmid DNA into E14 primary cortical neurons, a total of 3 μg of plasmid DNA and 4 μl Lipofectamine 2000 reagent were each diluted in 50 μl of OPTI-MEM™ (GIBCO-BRL), and applied to the cells cultured in 400 μl of NEUROBASAL with B27 supplement 3 h after plating. The medium was completely exchanged at 4.5 h after transfection, and cells were maintained in DMEM supplemented with D-glucose (4.5 g/l) and 10% fetal bovine serum. NIH3T3 cells stably expressing ephrin-A1 and 293T cells stably expressing EphB2 were established by transfection of pAlterMax encoding EphA2 or EphB2 as described above. Cells were cultured and selected in DMEM containing puromycin at a concentration of 2 μg/ml (for 293T cells) or G418 (Gibco BRL) at 0.6 mg/ml (for NIH3T3 cells) for 2–3 weeks. Well-isolated colonies were characterized further.

Immunoprecipitation and affinity precipitation

Transfected cells were harvested 48 h after transfection, and cell lysates were prepared with protease inhibitors in TXB buffer (10 mM Tris (pH 7.6), 150 mM NaCl, 5 mM EDTA (pH 8.0), 10% glycerol, 1 mM Na_3VO_4 and 1% Triton X-100). Whole brain tissue from E14 DDY mice was also lysed in TXB buffer with a Dounce homogenizer. The lysates were precleared by incubating them with protein G agarose (Boehringer Mannheim) for 1 h at 4°C. To purify the proteins, 1 μg of monoclonal or affinity-purified polyclonal antibodies was added and incubated with 500 μl of cell lysate for 1 h at 4°C. The antibodies were precipitated with protein G agarose for 2 h at 4°C. Immunoprecipitates were extensively washed with TXB buffer, separated by SDS–polyacrylamide gel electrophoresis (PAGE) and immunoblotted.

Affinity precipitation with GST-PBD was performed as described previously (Otsuki *et al*, 2001). Briefly, 293T cells were lysed in the lysis buffer (20 mM Tris–HCl (pH 7.5), 150 mM NaCl, 20 mM $MgCl_2$, 1 mM Na_3VO_4, 5% Triton X-100, 5 μg/ml aprotinin and 1 mM PMSF), and incubated with GST-PBD on sepharose for 1 h at 4°C. The precipitants were washed four times in the same buffer, and endogenous Rac1 protein was detected by immunoblotting.

In vivo phosphate labeling

Plasmids encoding Myc-tagged Tiam1 with ephrin-B1 or EphA2 were transfected into 293T cells in a 35 mm diameter dish. At 48 h after transfection, the transfected cells were cocultured with cells stably expressing EphB2 K661M or ephrin-A1. Transfected cells were preincubated in phosphate-free medium (GIBCO-BRL) for 15 h, and then coculture was performed in 0.5 ml of phosphate-free MEM containing 0.09 mCi of $^{32}P_i$ (NEN) for a further 4 h. The cells were lysed in the lysis buffer (20 mM Tris–HCl (pH 7.5), 150 mM NaCl, 20 mM $MgCl_2$, 1 mM Na_3VO_4, 0.5% Triton X-100, 5 μg/ml aprotinin and 1 mM PMSF). Myc-tagged Tiam1 was purified by immunoprecipitation using an anti-Myc antibody and separated on SDS–PAGE. $^{32}P_i$-labeled Tiam1 was visualized with a Bio Imaging Analyzer (BAS1000, Fuji) (lanes 1 and 2).

Cell staining

To examine the localization of Tiam1 after activation of ephrin-B1 or EphA2, cortical neurons from E14 DDY mice or NB1 cells were seeded on chamber slides. Cells were incubated with 4 μg/ml of clustered EphB2-Fc or ephrin-A1-Fc for 10 min, and then the medium was removed and further incubated in DMEM containing 10% FBS for the indicated period. Cells were fixed for 5 min at room temperature with 4% paraformaldehyde (PFA) in PBS and permeabilized for 5 min with 0.2% Triton X-100. The cells were preincubated in 2% BSA with 5% normal serum for 1 h, and incubated with the FITC-conjugated anti-Fc fragment of IgG antibody for 1 h at room temperature. In some experiments, cells were further stained for Tiam1 protein by sequential incubation with anti-Tiam1 (C-16) antibody and rhodamine-conjugated secondary antibody for 1 h for each. Photos were taken with Radiance 2100 confocal microscope (BioRad).

Neurite elongation assay

Plates and glass chamber slides were coated with Fc fusion proteins, by being filled with 5 μg/ml of Fc fusion proteins or the control Fc fragment plus 50 μg/ml of goat anti-IgG Fc (ICN) in sterile PBS(−) with gentle rocking for 1–2 h at room temperature before the protein solution was aspirated. Plates and chamber slides were washed three times with sterile PBS, and then incubated in PBS containing 2% (w/v) BSA for 30 min at room temperature to block the remaining protein-binding sites. Cortical neurons from the E14 mouse embryos were plated on the coated surface, and then fixed in 4% PFA in PBS after 20 h of incubation. In some experiments, cortical neurons were transfected with EGFP-tagged plasmids indicated as described above 3 h after plating on chamber slides, and then fixed after 20 h of transfection. For the statistical calculations, cells bearing neurites longer than one or three cell bodies in length were considered as cells with neurite outgrowth. In counting, only cells positive for EGFP were included in the analysis.

Supplementary data

Supplementary data are available at *The EMBO Journal* Online.

Acknowledgements

We thank Drs T Pawson (Mount Sinai Hospital), R Klein (European Molecular Biology Laboratory), N Kawazoe and N Nakaya (Laboratory of Biological Chemistry, School of Pharmaceutical Sciences, Showa University), M Hoshino (Department of Pathology and Tumor Biology, Graduate School of Medicine, Kyoto University) and Y Dobashi (Yamanashi University) for providing plasmids and cells used in this study. We thank Dr Ueki (First Department of Anatomy, Hamamatsu University School of Medicine) for assisting with the primary neuron culture technique from mouse embryos, and Associate Prof. Yamamoto (Laboratory of Cell Imaging, Photon Medical Research Center, Hamamatsu University School of Medicine) for assisting with the operation of the fluorescent microscope. We thank Prof. Nakahara (Department of Psychology, Hamamatsu University School of Medicine) for careful reading of this paper. We thank Prof. Sato (First Department of Anatomy, Hamamatsu University School of Medicine), Prof. Tsutsui and Dr Kosugi (Second Department of Pathology, Hamamatsu University School of Medicine) for useful discussion. This work was supported by the Smoking Research Foundation, Grants-in-Aid for Cancer Research from the Ministry of Health and Welfare of Japan, a Grant-in Aid-for Scientific Research (B, 10470056) on Priority areas (C-2, 12218215; C-2, 13216044), and COE (Medical Photonics, Hamamatsu University School of Medicine) from the Ministry of Education, Culture, Sports Technology and Science of Japan, and a Grant-in Aid-for Scientific Research (C2, 14570183) from the Japan Society for the Promotion of Science.

References

Birgbauer E, Oster SF, Severin CG, Sretavan DW (2001) Retinal axon growth cones respond to EphB extracellular domains as inhibitory axon guidance cues. *Development* **128**: 3041–3048

Cheng HJ, Nakamoto M, Bergemann AD, Flanagan JG (1995) Complementary gradients in expression and binding of ELF-1 and Mek4 in development of the topographic retinotectal projection map. *Cell* **82**: 371–381

Cowan CA, Henkemeyer M (2002) Ephrins in reverse, park and drive. *Trends Cell Biol* **12**: 339–346

Fleming IN, Elliott CM, Exton JH (1998) Phospholipase C-γ, protein kinase C and Ca^{2+}/calmodulin-dependent protein kinase II are involved in platelet-derived grpwth factor-induced phosphorylation of Tiam1. *FEBS Lett* **429**: 229–233

Fleming IN, Gray A, Downes CP (2000) Regulation of the Rac1-specific exchange factor Tiam1 involves both phosphoinositide

3-kinase-dependent and-independent components. *Biochem J* **351:** 173–182

Gao PP, Sun CH, Zhou XF, DiCicco-Bloom E, Zhou R (2000) Ephrins stimulate or inhibit neurite outgrowth and survival as a function of neuronal cell type. *J Neurosci Res* **60:** 427–436

Gao PP, Yue Y, Cerretti DP, Dreyfus C, Zhou R (1999) Ephrin-dependent growth and pruning of hippocampal axons. *Proc Natl Acad Sci USA* **96:** 4073–4077

Gao PP, Yue Y, Zhang JH, Cerretti DP, Levitt P, Zhou R (1998) Regulation of thalamic neurite outgrowth by the Eph ligand ephrin-A5: implications in the development of thalamocortical projections. *Proc Natl Acad Sci USA* **95:** 5329–5334

Gao PP, Zhang JH, Yokoyama M, Racey B, Dreyfus CF, Black IB, Zhou R (1996) Regulation of topographic projection in the brain: Elf-1 in the hippocamposeptal system. *Proc Natl Acad Sci USA* **93:** 11161–11166

Habets GG, Scholtes EH, Zuydgeest D, van der Kammen RA, Stam JC, Berns A, Collard JG (1994) Identification of an invasion-inducing gene, Tiam-1, that encodes a protein with homology to GDP-GTP exchangers for Rho-like proteins. *Cell* **77:** 537–549

Henkemeyer M, Orioli D, Henderson JT, Saxton TM, Roder J, Pawson T, Klein R (1996) Nuk controls pathfinding of commissural axons in the mammalian central nervous system. *Cell* **86:** 35–46

Holash JA, Soans C, Chong LD, Shao H, Dixit VM, Pasquale EB (1997) Reciprocal expression of the Eph receptor Cek5 and its ligand(s) in the early retina. *Dev Biol* **182:** 256–269

Kawauchi T, Chihama K, Nabeshima Y, Hoshino M (2003) The *in vivo* roles of STEF/Tiam1, Rac1 and JNK in cortical neuronal migration. *EMBO J* **22:** 4190–4201

Knoll B, Zarbalis K, Wurst W, Drescher U (2001) A role for the EphA family in the topographic targeting of vomeronasal axons. *Development* **128:** 895–906

Kunda P, Paglini G, Quiroga S, Kosik K, Caceres A (2001) Evidence for the involvement of Tiam1 in axon formation. *J Neurosci* **21:** 2361–2372

Leeuwen FN, Kain HE, Kammen RA, Michiels F, Kranenburg OW, Collard JG (1997) The guanine nucleotide exchange factor Tiam1 affects neuronal morphology; opposing roles for the small GTPases Rac and Rho. *J Cell Biol* **139:** 797–807

Liebl DJ, Morris CJ, Henkemeyer M, Parada LF (2003) mRNA expression of ephrins and Eph receptor tyrosine kinases in the neonatal and adult mouse central nervous system. *J Neurosci Res* **71:** 7–22

Mann F, Ray S, Harris W, Holt C (2002) Topographic mapping in dorsoventral axis of the *Xenopus* retinotectal system depends on signaling through ephrin-B ligands. *Neuron* **35:** 461–473

Matsuo N, Hoshino M, Yoshizawa M, Nabeshima Y (2002) Characterization of STEF, a guanine nucleotide exchange factor for Rac1, required for neurite growth. *J Biol Chem* **277:** 2860–2868

Otsuki Y, Tanaka M, Yoshii S, Kawazoe N, Nakaya K, Sugimura H (2001) Tumor metastasis suppressor nm23H1 regulates Rac1 GTPase by interaction with Tiam1. *Proc Natl Acad Sci USA* **98:** 4385–4390

Palmer A, Zimmer M, Erdmann KS, Eulenburg V, Porthin A, Heumann R, Deutsch U, Klein R (2002) Ephrin B phosphorylation and reverse signaling: regulation by Src kinases and PTP-BL phosphatase. *Mol Cell* **9:** 725–737

Pandey A, Lazar DF, Saltiel AR, Dixit VM (1994) Activation of the Eck receptor protein tyrosine kinase stimulates phosphatidylinositol 3-kinase activity. *J Biol Chem* **269:** 30154–30157

Sander EE, van Delft S, ten Klooster JP, Reid T, van der Kammen RA, Michiels F, Collard JG (1998) Matrix-dependent Tiam1/Rac signaling in epithelial cells promotes either cell-cell adhesion or cell migration and is regulated by phosphatidylinositol 3-kinase. *J Cell Biol* **143:** 1385–1398

Shamah SM, Lin MZ, Goldberg JL, Estrach S, Sahin M, Hu L, Bazalakova M, Neve RL, Corfas G, Debant A, Greenberg ME (2001) EphA receptors regulate growth cone dynamics through the novel guanine nucleotide exchange factor ephexin. *Cell* **105:** 233–244

Stam JC, Sander EE, Michiels F, van Leeuwen FN, Kain HE, van der Kammen RA, Collard JG (1997) Targeting of Tiam1 to the plasma membrane requires the cooperative function of the N-terminal pleckstrin homology domain and an adjacent protein interaction domain. *J Biol Chem* **272:** 28447–28454

Stuckmann I, Weigmann A, Shevchenko A, Mann M, Huttner WB (2001) Ephrin B1 is expressed on neuroepithelial cells in correlation with neocortical neurogenesis. *J Neurosci* **21:** 2726–2737

Tanaka M, Kamo T, Ota S, Sugimura H (2003) Association of Dishevelled with Eph tyrosine kinase receptor and ephrin mediates cell repulsion. *EMBO J* **22:** 847–858

Ueki T, Nakanishi K, Asai K, Okouchi Y, Isobe I, Eksioglu YZ, Kato T, Kohno K (1993) Neurotrophic action of gliostatin on cocultured neurons with glial cells. *Brain Res* **622:** 299–302

Wahl S, Barth H, Ciossek T, Aktories K, Mueller BK (2000) Ephrin-A5 induces collapse of growth cones by activating Rho and Rho kinase. *J Cell Biol* **149:** 263–270

Walker-Daniels J, Riese DJ, Kinch MS (2002) c-Cbl-dependent EphA2 protein degradation is induced by ligand binding. *Mol cancer Res* **1:** 79–87

Wang Y, Ota S, Kataoka H, Kanamori M, Li Z, Band H, Tanaka M, Sugimura H (2002) Negative regulation of EphA2 receptor by Cbl. *Biochem Biophys Res Commun* **296:** 214–220

Yun ME, Johnson RR, Antic A, Donoghue MJ (2003) EphA family gene expression in the developing mouse neocortex: regional patterns reveal intrinsic programs and extrinsic influence. *J Comp Neurol* **456:** 203–216

Zantek ND, Azimi M, Fedor-Chaiken M, Wang B, Brackenbury R, Kinch MS (1999) E-cadherin regulates the function of the EphA2 receptor tyrosine kinase. *Cell Growth Differ* **10:** 629–638

Zimmer M, Palmer A, Kohler J, Klein R (2003) EphB-ephrin-B bi-directional endocytosis terminates adhesion allowing contact mediated repulsion. *Nat Cell Biol* **5:** 869–878

FEBS 28948

FEBS Letters 577 (2004) 339–344

Analysis of estrogen receptor α signaling complex at the plasma membrane

Kotaro Azuma[a,b], Kuniko Horie[c], Satoshi Inoue[b,c], Yasuyoshi Ouchi[b], Ryuichi Sakai[a,*]

[a]*Growth Factor Division, National Cancer Center Research Institute, 5-1-1 Tsukiji, Chuo-ku, Tokyo 104-0045, Japan*
[b]*Department of Geriatric Medicine, Graduate School of Medicine, The University of Tokyo 7-3-1, Hongo, Bunkyo-ku, Tokyo 113-8655, Japan*
[c]*Division of Gene Regulation and Signal Transduction, Research Center for Genomic Medicine, Saitama Medical School, Hidaka-shi, Saitama 350-1241, Japan*

Received 11 August 2004; revised 28 September 2004; accepted 11 October 2004

Available online 21 October 2004

Edited by Veli-Pekka Lehto

Abstract There is accumulating evidence that the estrogen receptor (ER) can transduce specific signals at the plasma membrane. We tried to clarify the biological function of ER as a signaling molecule by identifying proteins that interact with the membrane-localized ER. The activation function 1 and 2 (AF-1 and AF-2) domains of ERα with or without the membrane-targeting sequence were stably expressed in the breast cancer cell line, MCF-7. The level of tyrosine phosphorylation of AF-2 was significantly elevated by the membrane localization. By mass-spectrometry analysis, α- and β-tubulins and heat shock protein 70 were identified as the AF-1-associated proteins. Of these, tubulins are associated only with membrane-targeted AF-1.

Keywords: Estrogen receptor; Non-genomic action; Breast cancer; Tubulin; Heat shock protein 70; Tyrosine phosphorylation

1. Introduction

Estrogen plays an important role not only in physiological processes such as the development of the female organs, reproduction, bone metabolism, and vascular dilatation, but also in pathological processes such as the development of breast cancer. Human estrogen receptor α (ERα) is a member of the nuclear receptor superfamily and functions as a ligand-dependent transcription factor [1,2]. A typical nuclear receptor contains a variable N-terminal region called activation function 1 (AF-1), a conserved DNA binding domain (DBD), a hinge region, and a C-terminal ligand binding domain called activation function 2 (AF-2). Both the AF-1 and AF-2 domains of ERα are shown to have a transcriptional activation function [3], and interact with transcriptional mediators and co-factors [4–10]. More than 80% of ERα is shown to localize in the nucleus in the absence of estrogen, and more than 95% is shown to localize in the nucleus upon estrogen stimulation [11]. Thus, it has been believed that the action of estrogen is mediated by nuclear-localizing ER through the regulation of target gene transcription.

However, there are accumulating evidences that the ER can transduce specific signals through association with other molecules outside the nucleus. In vascular endothelial cells, estrogen rapidly induces nitric oxide production by activating the PI3-kinase-Akt pathway [12]. In this process, ERα is shown to interact with the p85 subunit of PI3-kinase in a ligand-dependent manner [13]. In osteoblasts, ERα is shown to mediate the anti-apoptotic effect by activating the Src/Shc/Erk (extracellular signal-related kinase) pathway, and only the AF-2 domain expressed in the cytoplasm is necessary for this function [14]. These phenomena, called non-genomic actions, are not explained by the classical genomic action of ERα because of their rapid time course and the localization of interacting molecules, and are recognized as novel functions of the ER.

Independent laboratories have reported the non-genomic action of ERα in the breast cancer-derived cell line, MCF-7 [15,16]. They all observed that estrogen rapidly induces the phosphorylation of Erk, although different modes of action of ERα are proposed. Migliaccio et al. [15] showed that the association of ERα with non-receptor tyrosine kinase c-Src is the upstream event of ERα activation and the association of two molecules is dependent on the phosphorylation of Tyr 527 in the AF-2 domain of ERα. On the other hand, Song et al. demonstrated the direct association of ERα and adaptor protein Shc. This association was shown to use the AF-1 domain of ERα and does not require the phosphorylation of Tyr 527 [16]. It seems that the paucity of endogenous ERα at the plasma membrane makes it difficult to analyze the role of ERα at the membrane. In this study, we tried to clarify the components of the signaling complex in MCF-7 cells by the targeted expression of the ERα domain fragments at the plasma membrane.

2. Materials and methods

2.1. Plasmids

A FLAG epitope-tagged ERα AF-1 domain construct was generated by amplifying the coding sequence of human ERα by PCR using primers 5′-CGTACCTCGAGATGACCATGACCCCTCCACAC-3′

*Corresponding author. Fax: +81-3-3542-8170.
E-mail address: rsakai@gan2.res.ncc.go.jp (R. Sakai).

Abbreviations: AF-1 and AF-2 domains, activation function 1 and 2 domains; BSA, bovine serum albumin; DBD, DNA binding domain; DMEM, Dulbecco's Modified Eagle's medium; EGF, epidermal growth factor; ER, estrogen receptor; Erk, extracellular signal-related kinase; FBS, fetal bovine serum; Hsp70, heat shock protein 70; LC/MS/MS, liquid chromatography tandem mass spectrometry; WCL, whole cell lysate

0014-5793/$22.00
doi:10.1016/j.febslet.2004.10.025

and 5′-CGGGATCCTATTTGTCATCGTCGTCCTTGTAGTCCT-TGGCAGATTCCATAGCC- 3′. This resulted in a fragment with an *Xho*I site (underlined), a sequence that encodes the FLAG epitope (DYKDDDDK), followed by a termination codon and a *Bam*HI site (underlined). This fragment was then digested with *Xho*I and *Bam*HI sequentially, and ligated into mammalian expression vector pcDNA3.1(−)/Myc-His B (Invitrogen).

A membrane-targeted AF-1 domain construct was generated by PCR-based site-directed mutagenesis using the AF-1 construct as a template and primers 5′-GGTAGCAACAAGAGCAAGCCCAAG-GATGCCAGCCAGCGGACCATGACCCTCCACACC- 3′ and 5′-CATCTCGAGTCTAGAGGGC. The PCR product was then digested by *Dpn*I that degrades only methylated template plasmids. As a result, the N-terminal sequence of Src kinase (MGSNKSKPKDASQ encoded by underlined 39 bp) was inserted between the *Xho*I site and the N-terminal of AF-1.

A FLAG epitope-tagged ERα AF-2 domain construct was generated using the same procedure as that of the AF-1 construct by using primers 5′-CGTACCTCGAGGCCACCATGGGCAAGAAGAACA-GCCTGGCCTT-3′ and 5′-CGGGATCCTATTTGTCATCGTCGT-CCTTGTAGTCGACTGTGGCAGGGA-3′ (*Xho*I site and *Bam*HI site are underlined). A membrane-targeted AF-2 construct was also generated by PCR-based site-directed mutagenesis using the AF-2 construct as a template and primers 5′-GGTAGCAACAA-GAGCAAGCCCAAGGATGCCAGCCAGCGGAAGAAGAACA-GCCTGGCCTT- 3′ and 5′-CATGGTGGCCTCGAGTCTAG-3′.

2.2. Cell culture and transfection

MCF-7 cells were maintained in Dulbecco's Modified Eagle's medium (DMEM) with 10% FBS at 37 °C with 5% CO_2. When estrogen stimulation was necessary, MCF-7 cells were cultured in phenol red free DMEM with 5% Charcoal/Dextran Treated FBS (HyClone) for two days. Transfection was performed using FuGENE 6 (Roche) according to the manufacturer's instructions. Clones were selected using geneticin (Sigma) at a concentration of 800 μg/ml.

2.3. Antibodies and reagents

Anti-FLAG M2 monoclonal antibody and anti-α-tubulin antibody (B-5-1-2) were purchased from Sigma. Anti-β-tubulin monoclonal antibody (D-10) was from Santa Cruz. Anti-Hsp70 monoclonal antibody was purchased from Stressgen. Anti-phosphotyrosine antibody 4G10 was purchased from Upstate Biotechnology. Anti-ERα antibody (H-184) was purchased from Santa Cruz. FITC-conjugated anti-mouse antibody was from Santa Cruz. Alexa Fluor 488 goat anti-mouse IgG and Alexa Fluor 594 goat anti-rabbit IgG were purchased from Molecular Probe. HRP-conjugated anti-mouse antibody was purchased from Amersham Pharmacia. Protein-G Sepharose was purchased from Amersham Pharmacia, β-estradiol was purchased from Sigma. Nocodazole was from Sigma.

2.4. Immunocytochemistry

Cells were grown on microscope slides in 24-well plates, washed three times with PBS, fixed with 4% paraformaldehyde/0.1 M phosphate buffer for 4 min at room temperature, washed once with PBS, and permeabilized with 0.2% Triton X-100 in PBS. After another washing with PBS and blocking with 2% (bovine serum albumin, BSA)/TBST (100 mM Tris–HCl, pH 8.0, 150 mM NaCl, and 0.05% Tween 20) for 30 min, the cells were incubated with appropriate first antibodies in 2% BSA/TBST for 1 h at room temperature. The cells were washed three times with PBS and incubated with FITC-conjugated anti-mouse antibody (1:40) in 2% BSA/TBST. After the cells were washed three times with PBS, microscope slides were mounted in 1.25% DABCO and 50% PBS and 50% glycerol and visualized using a Radiance 2100 confocal microscope (Bio-Rad). In Fig. 4B, 3% BSA, 5% goat serum in TBS were used instead of 2% BSA in TBST. Alexa Fluor 488 goat anti-mouse IgG (1:2000) and Alexa Fluor 594 goat anti-rabbit IgG (1:2000) in 3% BSA and 5% goat serum/TBS were used as the secondary antibodies in Fig. 4B.

2.5. Immunoprecipitation and immunoblotting

Cells were lysed in 1% Triton X-100 buffer (50 mM HEPES, 150 mM NaCl, 10% glycerol, 1% Triton X-100, 1.5 mM $MgCl_2$, and 1 mM EGTA, 100 mM NaF, 1 mM Na_3VO_4, 10 μg/ml aprotinin, 10 μg/ml leupeptin, 1 mM phenylmethylsulfonyl fluoride), and the protein concentration was measured using BCA Protein Assay (Pierce).

For immunoprecipitation with anti-FLAG M2 antibody, cell lysate (2 mg/ml) was mixed with anti-FLAG affinity gel (Sigma) and rotated for 2–12 h at 4 °C. After the affinity gel was washed four times with 1% Triton X-100 buffer, FLAG-tagged proteins were eluted with 0.3 M glycin HCl at pH 3.5. The elutant was removed, neutralized with 2 M Tris–HCl (pH 8.8), and then boiled in the sample buffer (0.1 M Tris–HCl, pH 6.8, 2% SDS, 0.1 M dithiothreitol, 10% glycerol, and 0.01% bromophenol blue) for 5 min and analyzed by SDS–PAGE. The gels were transferred onto a polyvinylidene difluoride membrane (Millipore) and probed by immunoblotting. Immnunoreactive proteins were visualized with a chemiluminescence reagent (Western Lighting, Perkin Elmer).

2.6. Silver staining and LC/MS/MS analysis

The SDS–PAGE gels were silver stained according to a method used previously [17].

For liquid chromatography tandem mass spectrometry (LC/MS/MS) analysis, 12 ml of cell lysate containing 36 mg of total protein was mixed with 200 μl of anti-FLAG affinity gel and rotated for 8 h at 4 °C. The affinity gel was loaded onto a chromatography column (Bio-Rad), washed with 4 ml of 1% Triton X-100 buffer, and then eluted with 0.1 M glycin HCl at pH 3.5. The elutant was separated into several fractions in chronological order and then neutralized with 2 M Tris–HCl (pH 8.8). Aliquots of these fractions were subjected to SDS–PAGE analysis, stained with SYPRO Ruby protein gel stain (Bio-Rad), and fractions with a high concentration of FLAG-tagged protein were selected for further analysis. The selected fractions were dialyzed using EasySep (TOMY) in diluted (10%) PBS and then semi-lyophilized using a SpeedVac concentrator. The concentrated samples were subjected to SDS–PAGE analysis and the gel was stained with CBB (Bio-Rad). The bands to be analyzed were dissected, digested in gel with trypsin, and subjected to LC/MS/MS analysis.

3. Results

3.1. Establishment of cell lines stably expressing a series of domain fragments of ERα in MCF-7

To analyze molecules associated with ERα at the plasma membrane, a series of domain constructs were generated and named as shown in Fig. 1A. The FLAG epitope was attached to the C-terminus of the separated AF-1 domain and the AF-2 domain of ERα. They were named AF1 and AF2, respectively. To generate membrane-targeted constructs, the membrane-localizing sequence of c-Src kinase was added to the N-terminus of AF1 and AF2. Src kinase is a non-receptor tyrosine kinase localizing at the plasma membrane with its myristoylated N-terminal sequence. The membrane-targeted ERα domain constructs were named mAF1 and mAF2, respectively. ERα has a DBD and a hinge region between the AF-1 and AF-2 domains. Nuclear localizing signals are shown to reside in the DBD and hinge region [11]; therefore, these regions were excluded from our domain constructs to ensure cytoplasmic localization.

Stable transfectants that express each domain of ERα were then established using the breast cancer cell line, MCF-7. The expression and localization of the domain fragments were confirmed by the anti-FLAG staining of cells. It was observed that AF1 and AF2 localized diffusely in the cytoplasm (Fig. 1B: b and d), whereas mAF1 and mAF2 localized at the periphery of the cells (Fig. 1B: c and e), showing the obvious effect of the membrane-targeting sequence.

3.2. Tyrosine phosphorylation of the AF-2 domain at the plasma membrane

We next investigated the relationship between the tyrosine phosphorylation of the AF-2 domain and membrane locali-

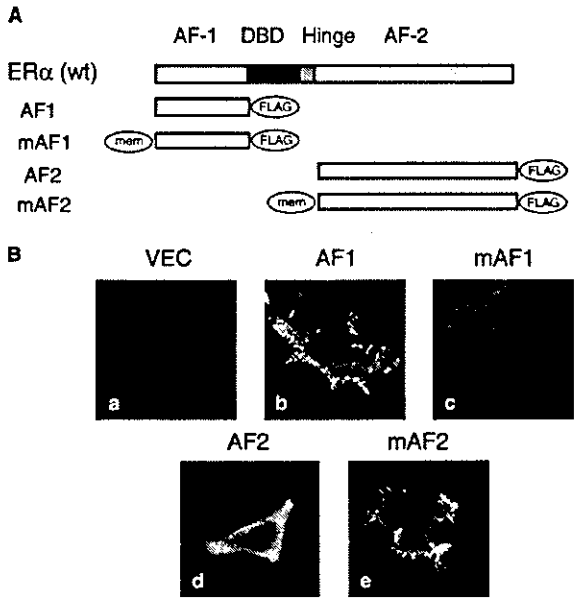

Fig. 1. Establishment of cell lines stably expressing a series of domain fragments of Erα in MCF-7. (A) Schematic representation of wild-type full-length ERα (wt), FLAG epitope-tagged AF-1 domain constructs with and without the membrane-targeting sequence (mem), and FLAG epitope-tagged AF-2 domain constructs with or without the membrane-targeting sequence. (B) Stable transfectants were immunostained with anti-FLAG antibody. (a) Empty vector; (b) AF1; (c) mAF1; (d) AF2; (e) mAF2. Cells were visualized with a confocal microscope at a magnification of 600×.

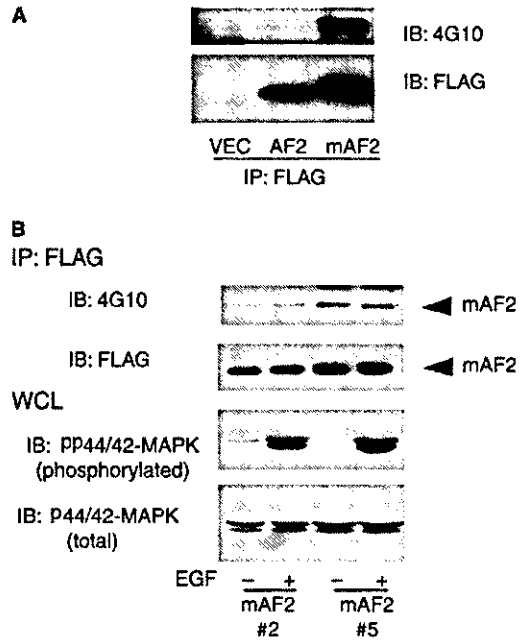

Fig. 2. Tyrosine phosphorylation of AF-2 domain at the plasma membrane. (A) Cell lysates of AF2 and mAF2 were immunoprecipitated with anti-FLAG antibody. Cells transfected with an empty vector (VEC) were used as a negative control. Each immunoprecipitate was subjected to immunoblotting analysis with anti-phosphotyrosine antibody 4G10 and anti-FLAG antibody. (B) Two independent clones of mAF2 (clones #2 and #5) were treated with either EGF (100 ng/ml) or distilled water for 5 min. mAF2 fragments were immunoprecipitated with anti-FLAG antibody and immunoblotted for 4G10 and anti-FLAG antibody. Whole cell lysates (WCLs) were immunoblotted with anti-phosphorylated p44/42 MAPK antibody and anti-p44/42 MAPK antibody.

zation using the stable transfectants we had established. The tyrosine phosphorylation of the mAF2 domain fragment was observed using phosphotyrosine specific antibody; however, almost no phosphorylation was detected in AF2 (Fig. 2A). This indicates that the AF-2 domain is phosphorylated exclusively at the plasma membrane.

To further characterize the tyrosine phosphorylation of the AF-2 domain, two independent clones of mAF2 cells were stimulated by EGF. In breast cancer cells, several tyrosine kinases, such as src family kinases [18,19] and Her-2 [20], have been reported to be transactivated upon EGF stimulation. However, no remarkable difference in the level of phosphorylation of mAF2 was observed upon EGF stimulation (Fig. 2B), suggesting that ERα is not the substrate of tyrosine kinases that is activated by EGF stimulation.

3.3. *Screening of the membrane-specific binding partners of the AF-1 and AF-2 domains*

In order to identify the interacting molecules with each domain of ERα, the lysates of the stable transfectants were purified with the anti-FLAG immunoaffinity column and analyzed by subsequent silver staining. Several candidates for mAF1-associated proteins were visualized by these procedures (Fig. 3). The bands around 200 kDa (arrowhead a), 50 kDa (arrowhead c) and 40 kDa (arrowhead d) were specifically seen in cells expressing mAF1, while the band around 70 kDa (arrowhead b) was observed in both cells expressing AF1 and cells expressing mAF1. None of these bands was co-purified with mAF2. These four bands were visible in the CBB gel stain from large-scale sample preparation. Two of these were successfully identified by LC/MS/MS analysis. The 50-kDa band that was specific to membrane-targeted AF1 was identified as β-tubulin (arrowhead c in Fig. 3). The 70-kDa band which was seen in both AF1 and mAF1 but not in mAF2 was identified as heat shock protein 70 (Hsp70) (arrowhead b in Fig. 3). Proteins specifically bound to mAF2 were not detected by this protocol (Fig. 3), although larger-scale purification was further attempted.

The association of mAF1 with β-tubulin was confirmed by immunoprecipitation followed by detection with β-tubulin antibody (Fig. 4A). This association was not detected in cells expressing AF1, indicating that this association is localized only at the plasma membrane. The absence of association between mAF2 and β-tubulin suggests that the association with β-tubulin was AF-1 domain-dependent and the membrane-targeting sequence did not serve as binding site for β-tubulin. A similar manner of association between mAF1 and α-tubulin was also detected (Fig. 4A), which is supported by the fact that β-tubulin forms heterodimers with α-tubulin.

To investigate physiological cooperation of tubulin and full-length endogenous ERα, immunocytostaining of MCF-7 cells was performed (Fig. 4B). Estrogen-dependent translocation of ERα to the plasma membrane was observed in 15 min on estrogen stimulation (Fig. 4B: h and k). At the same time, redistribution of α-tubulin was also observed at the plasma membrane (Fig. 4B: g and j). These two molecules showed co-localization in the superimposed image (Fig. 4B: i and l), which indicates possible association of these molecules in intact

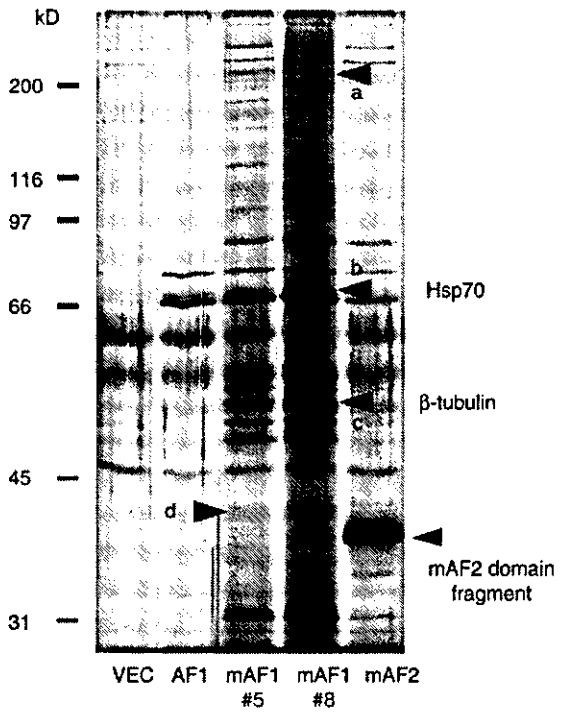

Fig. 3. Associated molecules to each domain fragment of ERα detected by silver staining. Each FLAG epitope-tagged domain fragment was immunoprecipitated by anti-FLAG antibody. One AF1 clone, two independent mAF1 clones (clones #5 and #8), and one mAF2 clone were analyzed. Immunoprecipitates were subjected to SDS–PAGE, and the gel was silver-stained. The two bands indicated by the arrowheads are Hsp70 and β-tubulin, which were identified later by LC/MS/MS analysis.

MCF-7 cells. These phenomena were not observed in the cells treated only by ethanol (Fig. 4B: d–f).

To further characterize the association of mAF1 and tubulins, cells expressing AF1 or mAF1 were treated with nocodazole, an inhibitor of tubulin polymerization. As a result, nocodazole treatment significantly blocked the association of mAF1 and α-tubulin (Fig. 4C). This indicates that mAF1 has higher affinity with polymerized microtubule filaments than with the depolymerized heterodimeric tubulin subunit.

Hsp70 was immunoprecipitated with both the AF1 and mAF1 domain fragments, but not with mAF2 (Fig. 4D). This suggests that the AF-1 domain is associated with Hsp70 outside the nucleus, but this association is not a membrane-specific event, in contrast with the case of tubulin.

4. Discussion

This study identifies polymerized tubulins as specific binding partners of the AF-1 domain of ERα at the plasma membrane using a breast cancer cell line, MCF-7. Hsp70 was also found to associate with the AF-1 domain although this association is not restricted at the plasma membrane. It was demonstrated that tyrosine phosphorylation of the AF-2 domain occurred within the plasma membrane, while the membrane-localized AF-2 domain failed to characterize any significant binding partners.

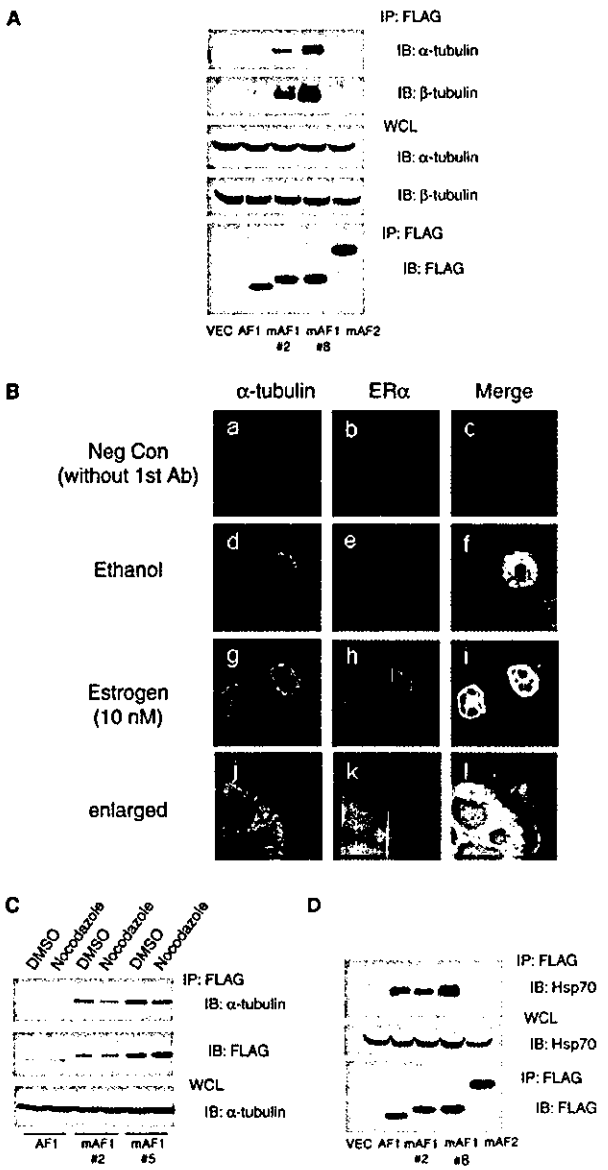

Fig. 4. Association of tubulins and Hsp70 with the AF-1 domain of ERα. (A) Cell lysates were immunoprecipitated and immunoblotted with anti-FLAG antibody, or anti-α- or β-tubulin antibodies as indicated. One AF1 clone, two independent mAF1 clones (clones #2 and #8), and one mAF2 clone were analyzed. (B) MCF-7 cells were treated with estrogen (10 nM) or ethanol (same concentration used in dilution of estrogen) for 15 min, then they were immunostained with anti-α-tubulin antibody (a, d, g, and j: green), and anti-ERα antibody (b, e, h, and k: red). Cells were visualized with a confocal microscope at a magnification of 600×. Superimposed confocal images (c, f, i, and l: merge) are also shown. Images without first antibodies (a–c) are shown as negative controls. Membranous area of estrogen stimulated MCF-7 cells was shown in magnified views (j–l: enlarged). (C) One AF1 clone and two independent mAF1 clones (clones #2 and #5) were treated with Nocodazole (33-μmol solution in DMSO) or DMSO (negative control) for 1 h. Cell lysates were immunoprecipitated and immunoblotted as indicated. (D) Cell lysates were immunoprecipitated and immunoblotted with anti-FLAG or anti-Hsp70 antibodies as indicated. One AF1 clone, two independent mAF1 clones (clones #2 and #8), and one mAF2 clone were analyzed.

It has been suggested by several independent laboratories that a subpopulation of ERα is associated with the plasma membrane and is responsible for the rapid effects of estrogen [15,16]. However, it appears that the subpopulation of membrane-associated ERα is considerably small, while the majority of ERα translocates into the nucleus upon estrogen stimulation. Therefore, we targeted the AF-1 and AF-2 domains of ERα to the plasma membrane to overcome the small amount of endogenous receptors at the plasma membrane.

The association of the AF-1 domain with polymerized tubulins or microtubules was specifically detected with the membrane-localized type of AF1, despite the wide distribution of microtubules throughout the cytoplasm. This result led us to conjecture that the association of ERα and microtubules is mediated by other molecules that reside at the membrane. Some signaling molecules are reported to associate with microtubules at the plasma membrane. p190RhoGEF (guanine nucleotide exchange factor) has a PH (pleckstrin homology) domain and localizes at the plasma membrane. This RhoA-activating molecule, which affects transcription and actin reorganization, has also been shown to interact directly with microtubules [21]. A small GTPase K-Ras, which can transduce signals to Erk, is another molecule shown to associate with microtubules at the plasma membrane [22]. It is possible that ERα forms a complex with K-Ras, microtubules and other unidentified molecules and affects the Ras signaling pathway. This may explain the rapid elevation of phosphorylated Erk on estrogen stimulation. The anti-tumor drug, paclitaxel, which is often used in the treatment. of breast cancer, has been shown to associate with polymerized microtubules and affect Ras-dependent signaling events [23]. This suggests that paclitaxel might also function by dissociating the signaling complex that involves ERα, K-Ras, and microtubules.

Association between the AF-1 domain and microtubules also tells us that microtubules are not used as tracks when ERα is transported to the plasma membrane, because the AF-1 domain needs to associate with microtubules at the cytoplasm before translocation if microtubules are used as tracks. Although membrane translocation is an important step for the non-genomic action of ERα, the precise mechanism is still elusive.

Ligand-dependent redistribution of both tubulins and ERα toward plasma membrane strongly suggests physical association between these molecules. To show the interaction of full-length ERα and tubulins, immunoprecipitation of tubulins or ERα was attempted several times using MCF-7 and Cos-7 cells. However, no association between tubulins and endogenous ERα was observed (data not shown). Immunocytostaining revealed that most of the full-length ERα was expressed in the nucleus and this situation was not improved even when membrane localizing sequence was attached to full-length ERα. Therefore, we concluded that our antibodies are not sensitive enough to detect the small population of membrane-localizing full-length ERα by immunoprecipitation.

It remains to be elucidated whether translocation of the small part of tubulins is a consequence of ERα translocation or an independent event. Nevertheless, this observation may indicate biological cooperation between ERα and tubulins.

It is also possible that the association of ERα and tubulins might contribute to the stabilization of microtubules, since mAF1 has higher affinity with polymerized tubulin and tubulin was well visualized at the plasma membrane when ERα was co-localized.

Hsp70 was shown to be another molecule that associates with the AF-1 domain expressed outside the nucleus. This association was not restricted at the membrane. The physiological role of the association between the AF-1 domain and Hsp70 is unclear. One possibility is that this association is involved in the degradation of cytoplasmic ERα. The glucocorticoid receptor, another member of the nuclear receptor superfamily, is shown to associate with Hsp90. CHIP, a U-box protein that has ubiquitin ligase activity, was shown to interact directly with Hsp90 and promote the degradation of glucocorticoid receptor [24]. CHIP was originally found as a Hsp70 interacting protein, and is also shown to localize outside the nucleus and to promote the degradation of Hsp70 bound protein [25]. Therefore, it is conceivable that in the case of ERα, Hsp70 mediates the degradation of cytoplasmic population of ERα. The degradation of ERα inside the nucleus was shown to be regulated differently depending on whether ERα is liganded or unliganded, and this mode of degradation generates a cyclic rhythm in the recruitment of ERα on estrogen-responsive promoters [26]. Hsp70 may be involved in the different regulation of ERα turnover outside the nucleus, which reflects the different functions of ERα outside the nucleus.

We also showed that tyrosine phosphorylation of the AF-2 domain occurs at the plasma membrane. It was previously reported that the AF-2 domain of ERα is phosphorylated on estrogen stimulation [15]. However, it was not clear whether the AF-2 domain is phosphorylated before or after membrane translocation. Our results favor the latter scenario. As the AF-2 domain without the membrane-targeted signal was not phosphorylated, the tyrosine kinases responsible for AF-2 phosphorylation localize strictly in the membranous area. Therefore, we assume that AF-2 phosphorylation does not regulate membrane translocation itself and that estrogen stimulation elicits the membrane translocation of ERα through interaction independent of phosphotyrosine.

So, what is the role of tyrosine phosphorylation of the AF-2 domain at the plasma membrane? Does phosphotyrosine mediate specific signals when the receptor translocates to the plasma membrane? Despite several attempts at purification, we have not yet identified the AF2-associated proteins. One of the factors that prevented the identification of the associated proteins was that the tyrosine-phosphorylated population of the AF-2 domain fragment was extremely small. The phosphorylation of the membrane-localized AF-2 domain was hardly detected by transient transfectants (data not shown). We managed to detect tyrosine phosphorylation of the membrane-localized AF-2 domain using stable transfectants. As long as the phosphorylated population of the membrane-localized AF-2 domain is small, only a small amount of molecules is supposed to bind to the AF-2 domain in a phosphotyrosine-dependent manner. This may be the reason that the previously reported association of membrane-localized AF-2 and c-Src [15] was not detected using our method (data not shown). Another possible factor that prevented the identification of the associated proteins is that AF-2 domain-bound proteins require the other domains of ERα to stabilize their association. In this case, longer ERα constructs would be needed to purify AF-2-associated proteins.